ISSN 0869-5938, Stratigraphy and Geological Correlation, 2019, Vol. 27, No. 7, pp. 804–839. © Pleiades Publishing, Ltd., 2019.

In loving memory of Vladimir Naumovich Beniamovsky, our colleague, friend, and mentor

Turonian–Coniacian Deposits of the Kamennyi Brod-1 Section (Southern Ulyanovsk-Saratov Trough)

E. M. Pervushov[a, *], I. P. Ryabov[a], A. Yu. Guzhikov[a], V. S. Vishnevskaya[c], L. F. Kopaevich[b], A. A. Guzhikova[a], E. A. Kalyakin[a], V. A. Fomin[a], V. B. Sel'tser[a], E. I. Il'inskii[a], G. V. Mirantsev[d], and P. A. Proshina[c]

[a] *Saratov State University, Saratov, 410012 Russia*
[b] *Moscow State University, Moscow, 119991 Russia*
[c] *Geological Institute, Russian Academy of Sciences, Moscow, 119017 Russia*
[d] *Paleontological Institute, Russian Academy of Sciences, Moscow, 117997 Russia*
**e-mail: pervushovem@mail.ru*

Received April 25, 2018; revised August 15, 2018; accepted October 25, 2018

Abstract—The most stratigraphically representative section of Turonian–Coniacian in the right-bank part of the Volga region is found at the Kamennyi Brod-1 section (Olkhovka district of Volgograd oblast). The subdivision of carbonate rocks into zones is based on the complexes of benthic foraminifera and other accompanying groups of invertebrates. Regressive-transgressive tendencies in the evolution of the Turonian–Coniacian basin is also reflected in the quantitative ratio between benthic and planktonic foraminifera. The earlier unknown representatives of Turonian and Coniacian marine biota are revealed: silicon sponges, crinoids, starfish, brittle stars, and brachiopods. The magnetostratigraphic (magnetopolar and petromagnetic) characteristic of the section is obtained, and the magnetic zone of anomalous polarity is revealed against the background of normal polarity (N). It is supposed that anomalous directions of magnetization represent the stabilized vector sum of oppositely directed components, one of which (corresponding to reverse polarity) is the primary one.

Keywords: Upper Cretaceous, Cenomanian, Turonian, Coniacian, Santonian, Volga River right bank of Volgograd oblast, biostratigraphy, magnetostratigraphy, petromagnetism

DOI: 10.1134/S0869593819070025

INTRODUCTION

In the southwestern part of the Ulyanovsk-Saratov trough, there are several sections with characterized (to different degree) intervals of Cenomanian, Turonian–Coniacian, and Santonian rocks (Fig. 1). In a stratigraphic sense, the most complete section of Turonian–Coniacian carbonate rocks is the Kamennyi Brod-1 one (hereinafter, KB-1; 49°44′15.9″ N, 44°23′18.0″ E). This is represented by trenches for pipelines with vertical walls and exposed chalk and marl on the right bank of the Ilovlya River (Fig. 2). Here microfaunal samples showed the presence of small echinoderms and brachiopods, in addition to foraminifera and radiolarians, whereas microfauna collected in each layer of dense marls did not yield the expected results (Figs. 3, 5–7).

The faunal characteristic of terrigenous (Cenomanian) and carbonate (Turonian) rocks from the KB-1 section was supplemented with the fossil data collected at such sections as Kamennyi Brod-2 (49°47′32.1″ N, 44°25′24.6″ E), Chukhonastovka-1 (49°51′15.2″ N, 45°06′9.3″ E), and Chukhonastovka-2 (49°51′12.5″ N, 45°05′26.9″ E). The Kamennyi Brod-2 (KB-2) section is a small sand quarry where only transitional Cenomanian–Turonian intervals of rocks are available for direct sampling. The distance between the KB-1 and KB-2 sections is 6 km (Fig. 1). Both Chukhonastovka sections are located at the distance of 52 km from the KB-1 section (Figs. 1, 4). The Chukhonastovka-1 section is a natural steep scarp composed of Cenomanian sands and Turonian marls, whereas the Chukhonastovka-2 section is an abandoned two-stage carbonate quarry with a broad and subflat upper stage.

The description of the section and a review of the history of study and structural position of the area under discussion, as well as determination of species of sponges, were provided by E.M. Pervushov. Benthic

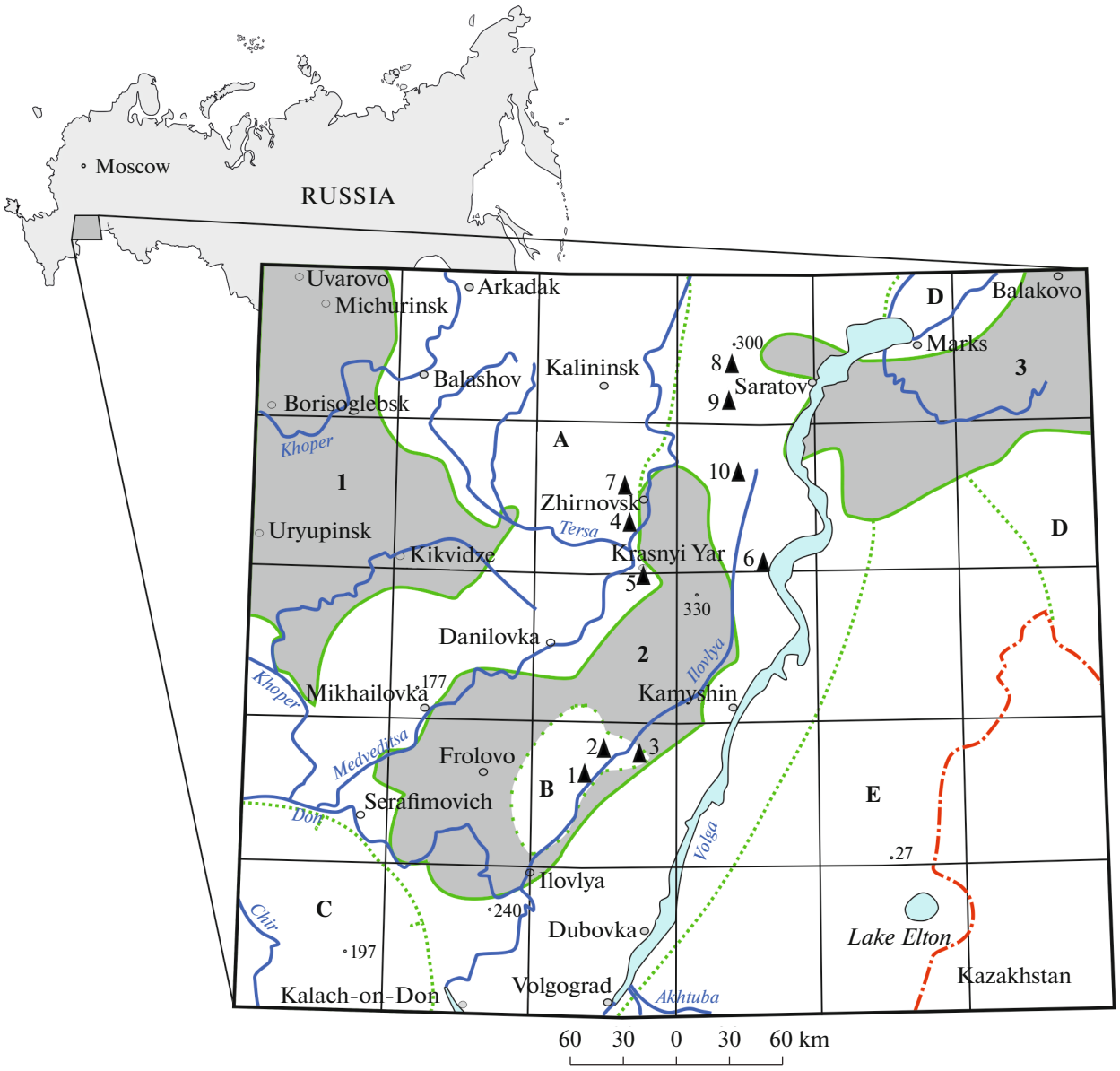

Areas of contemporary absence of Cretaceous deposits:
1. Voronezh syneclise
2. Don-Ilovlya (Don-Medveditsa) swell
3. Volgo-Uralian anteclise, Balakovo rise, and Stepnovo composite swell

Boundaries of structural-facial zones within sedimentation basin
A. Khoper monocline–Tersa depression
B. Ulyanovsk-Saratov trough (southwestern centricline) and Volga region monocline
C. Ukrainian syneclise (northeastern limb)
D. Ulyanovsk-Saratov trough (northeastern part) and Caspian syneclise (northern side)
E. Caspian syneclise (western side)

1▲ Geological sections: (1) Kamennyi Brod-1; (2) Kamennyi Brod-2; (3) Chukhonastovka; (4) Melovatka; (5) Krasnyi Yar; (6) Nizhnyaya Bannovka; (7) Bolshoy Kamennyi ovrag (Zhirnovsk town); (8) Ozerki; (9) Karamyshka; (10) Splavnukha

Fig. 1. Scheme of structural-facial zoning (Late Cretaceous) for the Lower Volga region (*Gosudarstvennaya*..., 2009) and locations of the studied Turonian–Coniacian sections.

Fig. 2. The Kamennyi Brod-1 section: (a) general view of pipeline trenches; (b) view of the southern trench from east; (c) northern wall of the southern trench.

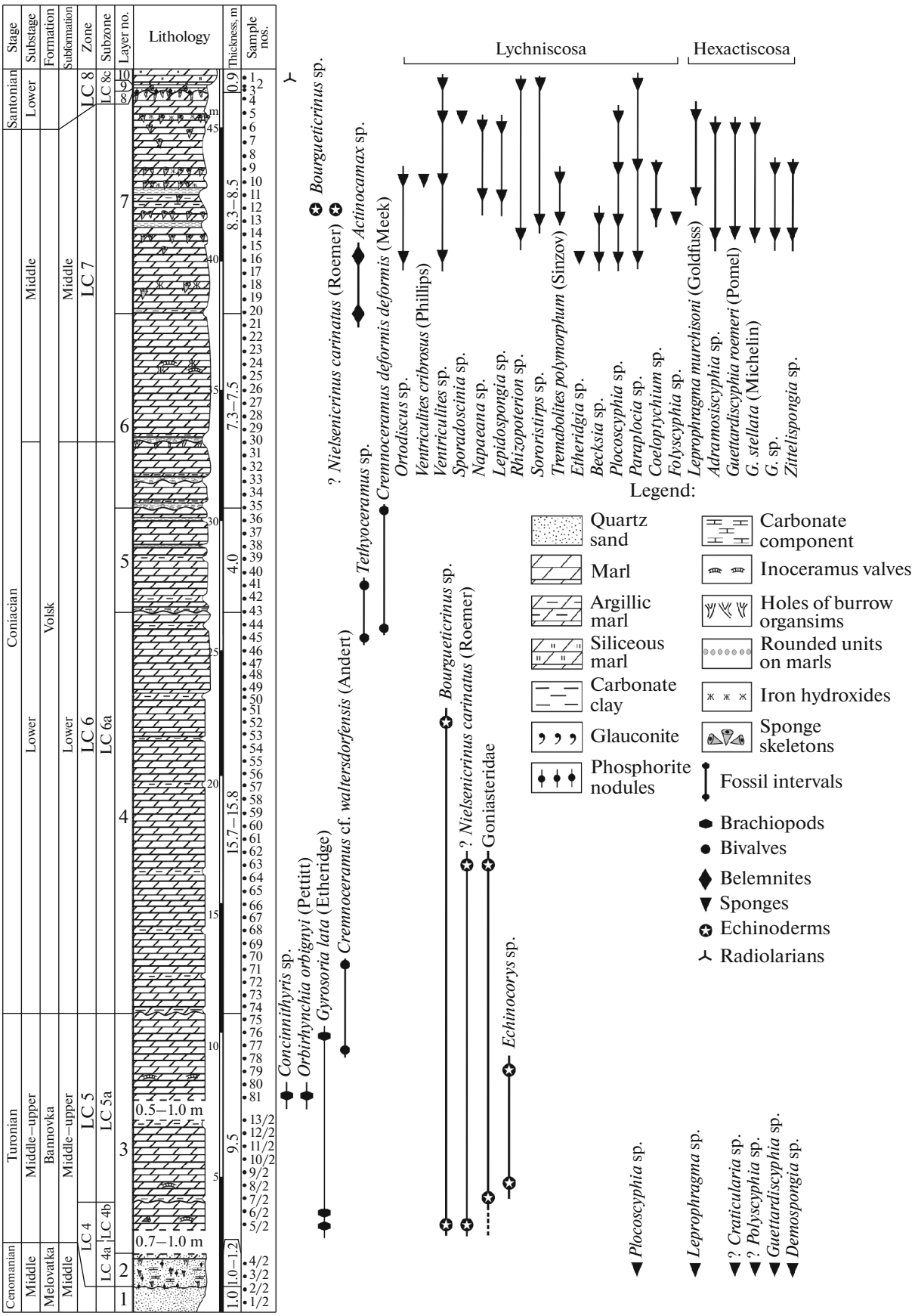

Fig. 3. Distribution of invertebrates in the KB-1 section. The BF-based zones and subzones (LC) are shown.

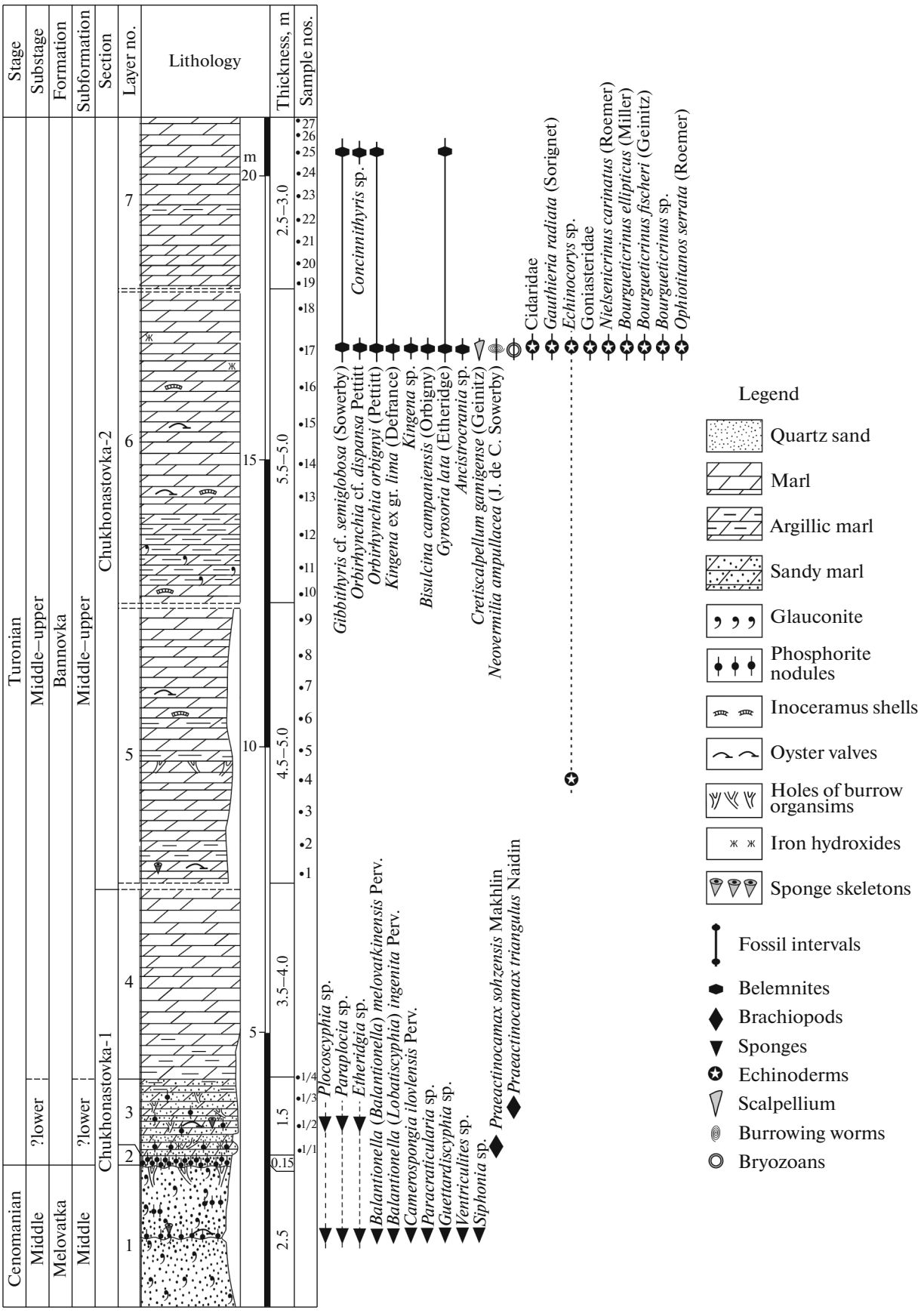

Fig. 4. Distribution of invertebrates in the Chukhonastovka-1 and Chukhonastovka-2 sections.

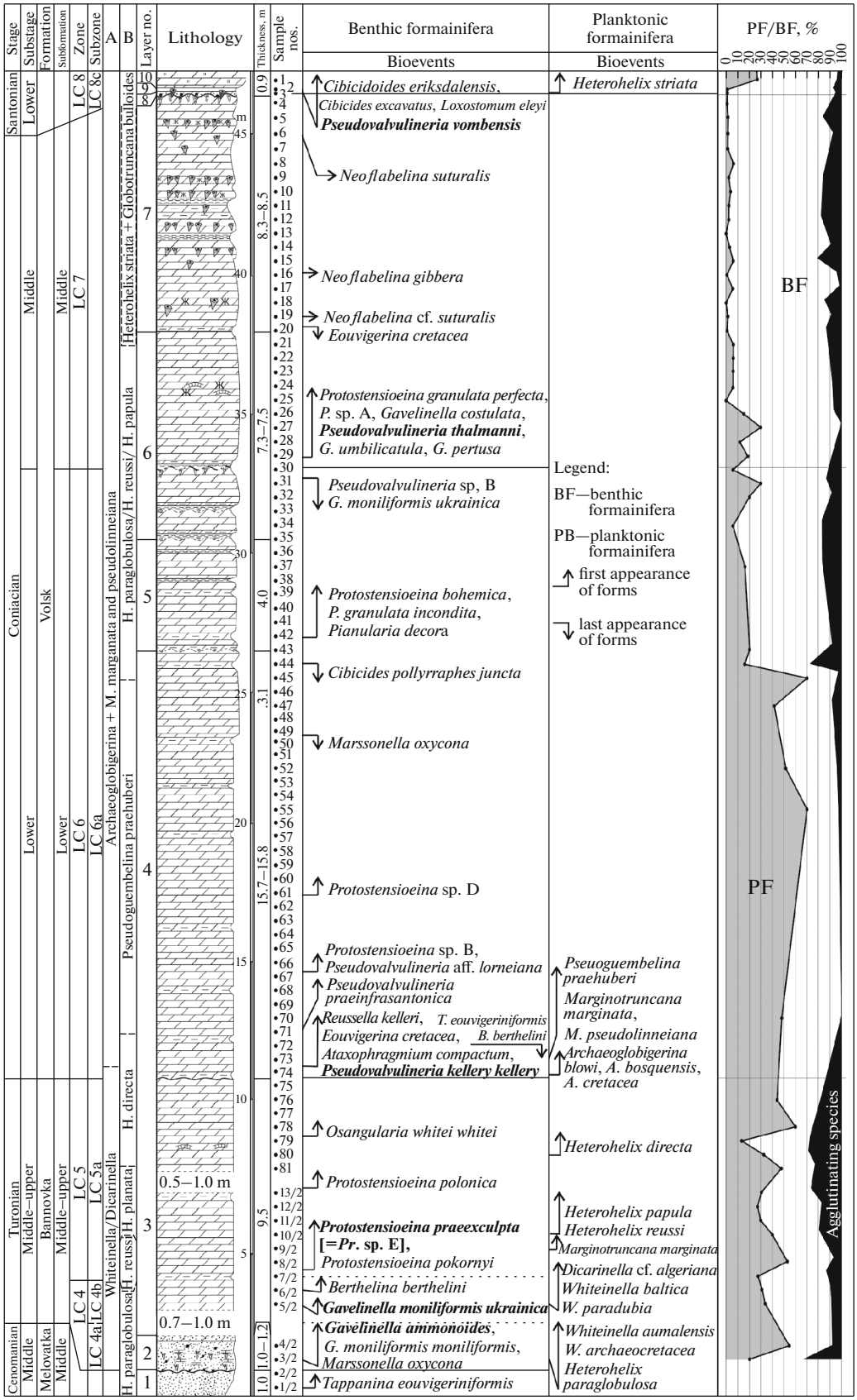

Fig. 5. Bioevents in the BF and PF communities as revealed from the studies of the KB-1 section. The BF-based zones and subzones (LC) and layers with globotruncanids (A) and heterohelicids (B) are shown. Legend to the lithologic column is the same as Fig. 3.

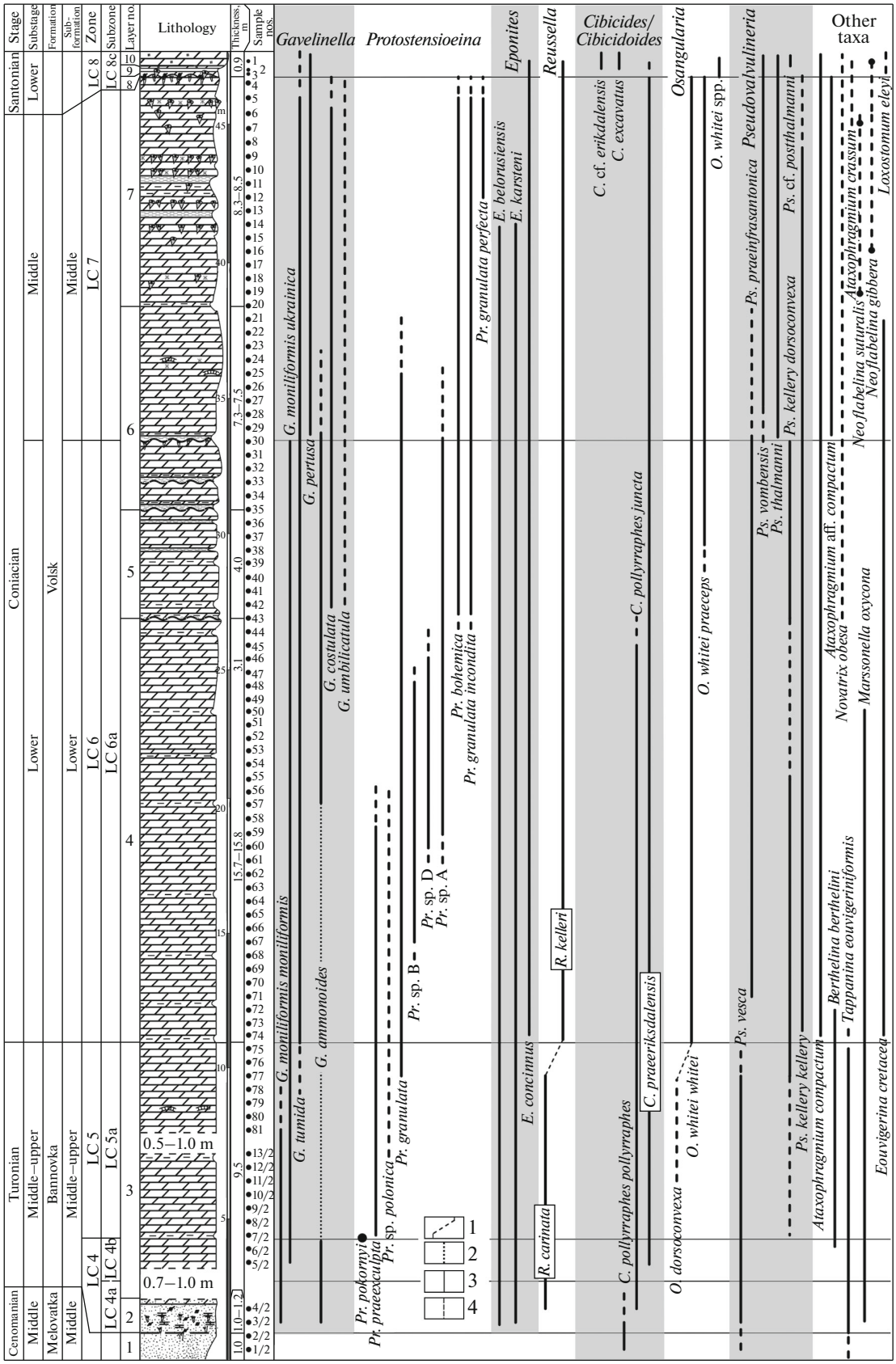

Fig. 6. BF distribution in the KB-1 section. The BF-based zones and subzones (LC) are shown. Legend: (1) transitional varieties, (2) species is not found in the interval, (3) ubiquitous species, (4) single occurrence of species. Legend to the lithologic column is the same as Fig. 3.

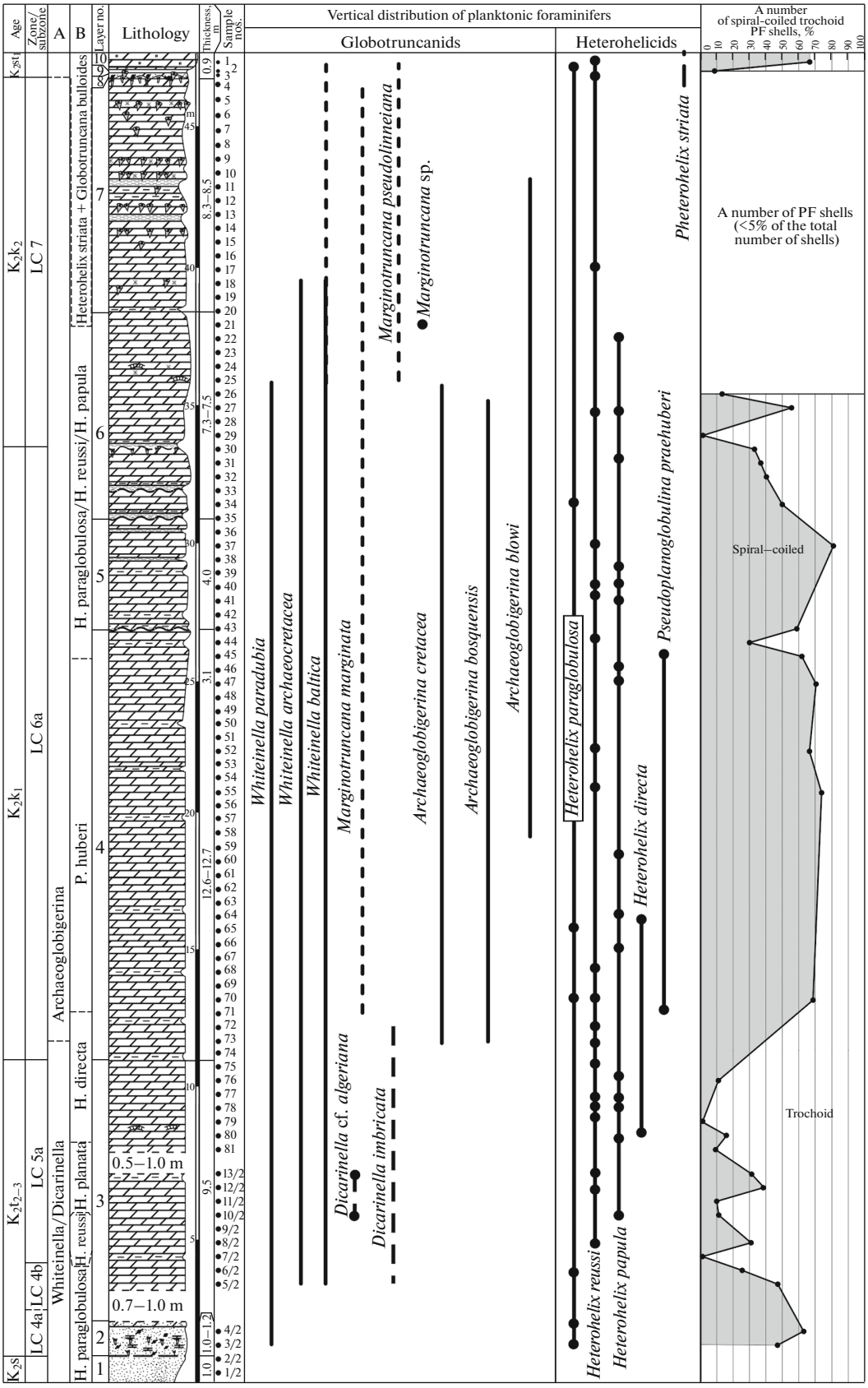

Fig. 7. PF distribution in the KB-1 section. The BF-based zones and subzones (LC) and layers with globotruncanids (A) and heterohelicids (B) are shown. Legend to the lithologic column is the same as Fig. 3.

foraminifera were analyzed by I.P. Ryabov; planktonic foraminifera, by L.F. Kopaevich and P.A. Proshina; radiolarians, by V.S. Vishnevskaya; bivalves and belemnites, by V.B. Sel'tser; brachiopods, by E.I. Il'inskii; echinoderms and crinoids, by E.A. Kalyakin; crinoids, starfish, and brittle stars, by G.V. Mirantsev; scalpellums, by A.S. Alekseev; and tubular worms, by A.P. Ippolitov. Paleomagnetic and petromagnetic studies were carried out by A.A. Guzhikova and A.Yu. Guzhikov. A.G. Manikin and V.A. Grishchenko participated in the field sampling of the section.

The study of the KB-1 section is an element of comprehensive research of stratigraphy of Turonian–Coniacian carbonate and terrigenous-carbonate rocks on the right bank of the Volga River region. At present, it is this section where the maximum thickness of Turonian–Coniacian carbonate rocks has been revealed, and moreover these rocks are accessible for direct sampling. The main aims of studies at the KB-1 section and associated geological objects were the following:

(1) substantiation of the Turonian–Coniacian boundary based on the analysis of macrofossil and microfossil distribution;

(2) distinguishing the stratigraphic units (substages) and detailed biostratigraphic units (biozones and subzones);

(3) determination of the stratigraphic extent of hiatuses in sedimentation at the base and top of Turonian–Coniacian carbonate rocks;

(4) correlation of biostratigraphic units distinguished in the KB-1 section and those identified in sections investigated within the limits of the right bank of the Volga River region (Guzhikov et al., 2017; Guzhikova et al., 2019; Pervushov et al., 2017a, 2017b; Surinskiy and Guzhikov, 2017) and the known ones in the Karamysh and Volsk depressions;

(5) obtaining magnetostratigraphic (magnetopolar and petromagnetic) characteristics of the section, in particular, in order to distinguish possible magnetic zones of anomalous polarity.

HISTORY OF STUDIES OF THE TURONIAN–CONIACIAN DEPOSITS ON THE RIGHT BANK OF LOWER VOLGA RIVER REGION

The first data on the structure of Upper Cretaceous deposits in the Ilovlya River basin were obtained at the beginning of the 20th century (Arkhangelsky, 1908, 1912; Arkhangelsky and Dobrov, 1913). Mazarovich (1924) estimated the local thickness of carbonate sequence at 36–44 m, assuming that its lower part was Turonian and the upper one was Coniacian, without the possibility of drawing a clear boundary, and marked the northern limit of extent of Coniacian rocks at the latitude of the village of Melovatka and city of Kamyshin. Milanovskii (1940) briefly characterized Cretaceous rocks on the right bank of Ilovlya River and described the index fossils for the Turonian (*Inoceramus lamarcki* Parkinson) and Coniacian ("*Inoceramus*" *involutus* Sowerby).

The directed study of Upper Cretaceous deposits in the Lower and Middle Volga regions was related to the geological survey here at the turn of the 1940s to 1950s (Morozov, 1951, 1956, 1962; Morozov and Bondareva, 1970; Morozov and Orekhova, 1969; Rykov, 1951a, 1951b). The Turonian–Coniacian rocks in this region were traditionally considered as a united geological body. In order to stratify the carbonate sequence, it was proposed to use external signs of selective alterations in lithology of rocks within its upper layers. The first results of microfaunal studies showed that the rocks where foraminifera reliably belonging to the Turonian disappeared could be ascribed to the Coniacian. Paleontological characteristics of the Coniacian rocks were obtained on the basis of rare findings of "*Inoceramus*" *involutus* Sowerby and the associated complex of foraminifera (Kamysheva-Elpatievskaya and Kuznetsova, 1951; Taboyakov, 1953). On the basis of the complex of foraminifera, the Coniacian Stage, with the lower and upper substages, was distinguished for the Lower Volga region for the first time (Baryshnikova, 1955, 1956, 1959; Baryshnikova et al., 1961). V.I. Baryshnikova distinguished a new species (*Stensioeina emscherica*), and now it is considered as a zonal fossil of the lower Coniacian (Beniamovsky, 2008a).

In the mid-1970s, special-purpose investigations of Upper Cretaceous reference sections in the Volga region were carried out. In the biostratigraphic characteristics of the considered stratigraphic units, the leading role was played by studies of foraminifera (Bondareva and Morozov, 1984). The authors of these studies supposed that Coniacian deposits are of local distribution and emphasized the possibility of distinguishing the base of this stage only from analysis of complexes of foraminifera. V.F. Saltykov (Saltykov and Pervushov, 2007a, 2007b) provided the mineralogical and lithologic characteristics of rocks from the Bannovka (Turonian) and Volsk (Coniacian) formations and also the thickness of these units on the basis of the data of mapping wells from the right bank of northern part of Volgograd oblast.

At present, enhanced methods and techniques, combined with the appearance of new instruments for petromagnetic and paleomagnetic studies, have made it possible to perform comprehensive biostratigraphic and magnetostratigraphic studies of the Turonian–Coniacian deposits (Guzhikov et al., 2017; Guzhikova et al., 2019; Pervushov et al., 2017a, 2017b). The approaches of cyclostratigraphic analysis were tested at the Turonian–Coniacian interval of the Nizhnyaya Bannovka section (Surinskiy and Guzhikov, 2017). The data on the sections from right bank part of the Volga region (Krasnyi Yar, Melovatka, Zhirnovsk, Nizhnyaya Bannovka, Splavnukha, and Ozerki) from the study give us ground to believe that Coniacian

units are characterized by a more widespread lateral distribution than was thought earlier.

MATERIALS AND METHODS

Carbonate rocks of the KB-1 section were studied in the southern wall of the southernmost of three trenches, in order to trace the continuous sequence of bedding for the upper and larger part of the studied units. The lower intervals of marls and transition to Cenomanian terrigenous rocks were studied at the base of the northern wall of the central trench. Various samples were collected in "sample-to-sample" manner with an interval of 0.5 m between them. Microfossils were extracted from 94 samples (Figs. 3, 5–7) by mixing with thiosulfate ($Na_2SO_4 \cdot 10H_2O$). Cleaning of shells became more effective after ultrasonic treatment of powders. Foraminifera were taken from fractions >0.1 mm with the use of an MBS-9 optical microscope. Foraminifera were imaged at the Laboratory for Materials Nanodiagnostics, Educational and Scientific Institute of Nanostructures and Biosystems, Saratov State University, with the use of a MIRA 2 LMU autoemission scanning electron microscope (Tescan).

We extracted the following definitive macrofossils from powders of microfaunal samples collected in individual intervals of marls: brachiopod shells, skeleton fragments of echinoderms echinoderms and bryozoans. Brachiopod shells were of microsize (2–3 mm), fine size (3–8 mm), and macrosize (10–25 mm) and of good primary preservation. The study of powders (fraction >0.4 mm) obtained upon maceration of samples allowed us to trace the distribution of crinoids in the KB-1 section (Fig. 3). The images of echinoderms were obtained at the Paleontological Institute of the Russian Academy of Sciences using Cambridge CAMSCAN-4 and TESCAN VEGA-II XMU scanning electron microscopes. We also employed the typification of burials of marine invertebrates by Sobetsky (1978).

For magnetostratigraphic studies, we collected oriented hand specimens from 109 stratigraphic levels. At the KB-1 observation point (o.p.), the sampling interval was 1 m; at o.p. no. 3124, it was 0.4 m (Fig. 8). When collecting the microfaunal samples with the interval of 0.5 m between them, we obtained 89 unoriented hand specimens for petromagnetic analysis. Each oriented hand specimen was cut into four cubic specimens 2 × 2 × 2 cm in size (with preserved orientation). Four analogous specimens each were obtained from the unoriented samples as well.

Petromagnetic studies were carried out in order to (a) assess the applicability of rocks to paleomagnetic studies, (b) perform additional subdivision of the section, and (c) to obtain nontrivial data on the conditions of formation of rocks. Petromagnetic studies implied measurements of magnetic susceptibility (K) and anisotropy of magnetic susceptibility (AMS), natural remanent magnetization ($\mathbf{J_n}$), parameters of magnetic saturation (remanent magnetization of saturation, $\mathbf{J_{rs}}$), remanent coercive force ($\mathbf{H_{cr}}$), and others, and also determination of the increment of magnetic susceptibility after heating specimens in a SNOL-6/11-V muffle furnace at 500°C for one hour (dK). Parameter K was measured using an MFK1-FB kappabridge; $\mathbf{J_n}$ was measured on a JR-6 spinner magnetometer and 2G-Enterprises cryogenic magnetometer (SQUID). For analyzing AMS data, Anisoft 4.2 software was used. Apart from the characteristics obtained experimentally, we calculated the Koenigsberger's parameter (Q factor, equivalent to the ratio between $\mathbf{J_n}$ and inductive magnetization) and $K/\mathbf{J_{rs}}$ ratio. Variations in magnetic properties were interpreted as changes in sedimentation conditions, in accordance with the principles developed earlier (Guzhikov, 2013; Molostovskii and Khramov, 1997).

Petromagnetic studies were carried out by the standard technique (Molostovskii and Khramov, 1997) implying measurements of $\mathbf{J_n}$ in oriented specimens on a JR-6 spinner magnetometer and cryogenic magnetometer after the series of sequential magnetic cleaning by an alternating field from 12 to 60 mT with the steps of 1–5 mT, depending on the dynamics of specimen demagnetization, at an LDA-3 AF installation. The component analysis of the obtained data was performed using Remasoft 3.0 software.

STRUCTURAL POSITION OF THE KAMENNYI BROD AND CHUKHONASTOVKA SECTIONS

The main events of the Turonian–Coniacian Stage in the present-day Volga region were the considerable northward expansion of dominating carbonate accumulation and appearance of subtropical marine invertebrates. These events were coupled with formation of the new structural plan of the territory: in its greater part, middle Turonian marls occur on middle or upper Cenomanian sands and silts; in the north, they superimpose Albian clays; and in the south, "they occur on rocks ranging from Carboniferous to Lower Triassic in age" (Morozov, 1962; Morozov and Orekhova, 1969). The lithologic uniformity of Turonian–Coniacian rocks was due to the fact they were considered as part of the Gubkino Horizon (*Gosudarstvennaya...*, 2009; Olfer'ev and Alekseev, 2005; *Stratigraficheskaya...*, 2004). The noticeable variations in lithology of rocks belonging to this stratigraphic interval were noted at the base ("surka") and in the periphery of the sedimentation basin in the Coniacian (terrigenous-carbonate units of the Borisoglebsk sequence) (Olfer'ev and Alekseev, 2005; Olfer'ev et al., 2007).

The preserved arches of non-elongated submeridional troughs are traced in isopach maps of the Gubkino Horizon in the southern part of the right bank of the Volgograd region (Morozov, 1962). To the north of

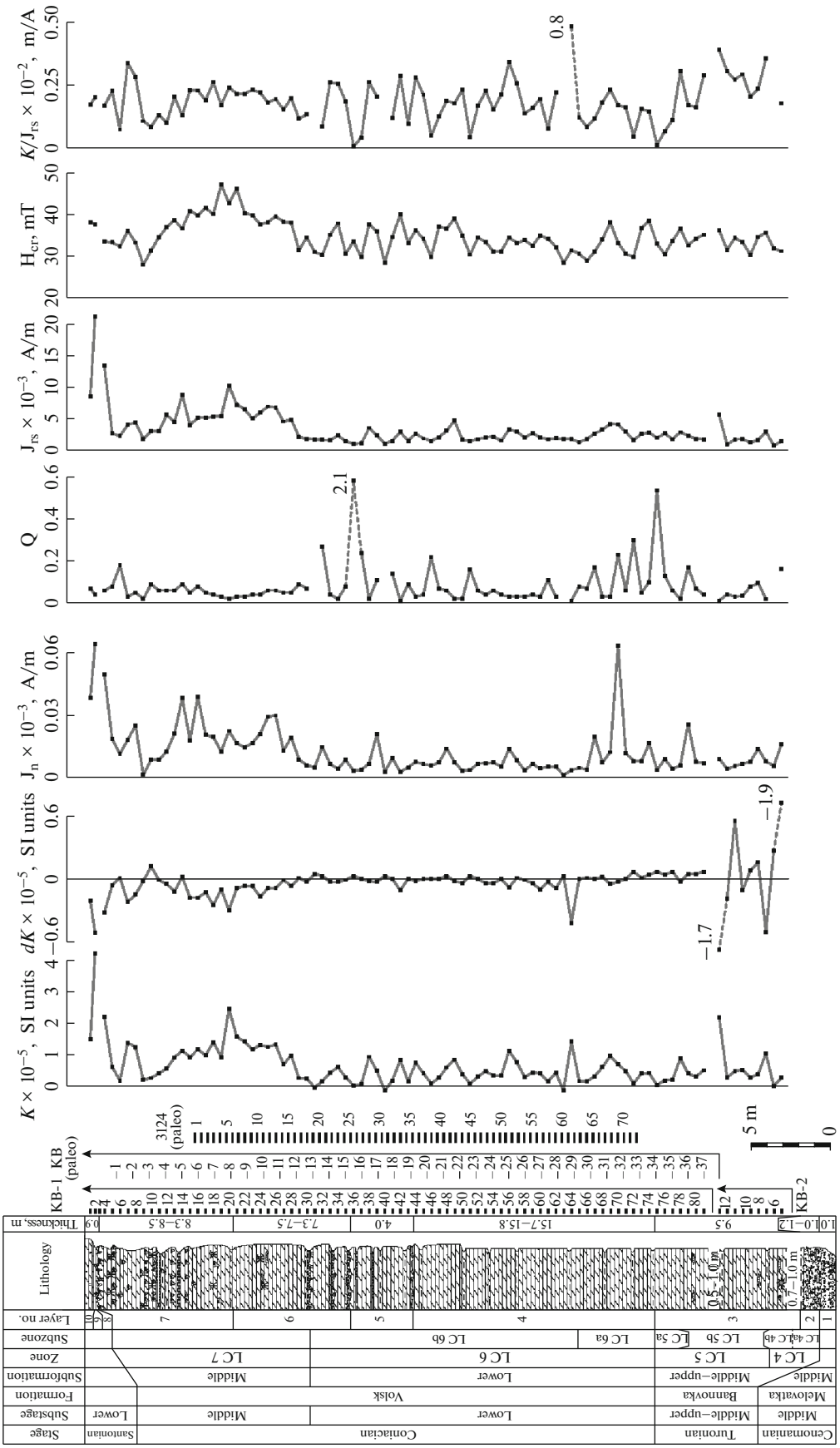

Fig. 8. Petromagnetic characteristic of the KB-1 section. Legend is the same as Fig. 3.

here, in the middle part of the Don–Medveditsa Swell, the arch of southwestern termination of the superimposed Ulyanovsk-Saratov trough is represented by a remnant of Upper Cretaceous rocks (*Geologicheskaya*..., 2009). This negative structure, known as the Lower Volga trough or Volgograd paleotrough (Saltykov and Pervushov, 2007a), confines the area of Coniacian rocks. The KB-1 and KB-2 sections are located in the central part and at its northern centricline, respectively, whereas the Chukhonastovka section is located in its eastern limb (Fig. 1).

It is supposed that to the north, west (Tersa depression), and east of the present-day Don–Medveditsa and Rtishchevo–Balandino swells, closer to the Near-Volga monocline and North Caspian depression, divergence of the most lowered parts of the trough took place. Perhaps, some middle submeridional trough exitsed here: it ran along the Karamysh depression and was limited by the sublatitudinal Elshanka–Sergievo and Tatishchevo swells in the north (Pervushov et al., 2017a). The known phase of maximal extent of the Lower Volga trough is associated with the Coniacian Stage. Taking the erosional cut in the pre-Santonian into account, the thickness of rocks in the Gubkino Horizon is up to 70 m to the south of Volgograd and about 50 m in the Kamennyi Brod section, decreasing to 8 and 2 m in the Ozerki and Karamyshka sections, respectively. In the northwestern wing of the Don–Medveditsa swell and in the Tersa depression, the thickness of chalk-and-marl sequence is up to 25–35 m, whereas the thickness of Coniacian rocks is estimated to be no thicker than a few meters (Saltykov and Pervushov, 2007a, 2007b). Eastward, the thickness of Coniacian carbonate rocks also decreases to about 4–5 m in the Nizhnyaya Bannovka section and to 10 m on the northern side of the North Caspian depression (Sedaikin et al., 1969).

In chalk quarries of the stratotypical area (Volsk depression), there are intervals of Middle–Upper Coniacian rocks with thickness of up to 2–4 m, identified from microfossils and inoceramids. In the KB-1 section, Coniacian marls are up to 35–36 m thick.

Description of the KB-1 Section

From bottom to top, the KB-1 section includes the following layers (Fig. 3).

Layer 1. Quartz medium-grained light gray and yellowish sand with rare large quartz grains and indistinct lamination. Transition to the overlying layer is gradual, traced owing to the increasing content of carbonate material of higher density and darker tones. Visible thickness is 0.7–1 m.

Layer 2. Carbonate sand nonuniformly marked with spots of iron hydroxides along many multidirected channels. In the lower part, sand is loose, whereas in the upper part it is dense; closer to the top, sand transits to sandy gray marl with yellow spots coinciding with fossil fragments and channels. Weakly phosphated dark gray and brown carbonate nodules up to 2–3 cm in diameter are uniformly scattered over the layer. Rarely, fine brown and black well-rounded phosphorite impregnations of up to 1.5–3 cm in size are seen. Locally silicified parts along channels are dark gray and blue in color. Large terrigenous elements in rocks form elongated lenses containing teeth of shark-like fishes and rounded skeletons of fine Hexactinnelida sponges (*Camerospongia ilovlensis* Perv., *Craticularia* sp., *Guettardiscyphia* sp., *Leptophragma* sp., *Ploscoscyphia* sp.). Visible thickness is up to 1.0–1.2 m.

Layer 3. Light gray dense indistinctly laminated marl. In the lower part, marl is tabular and massive, 1.9–2.0 m thick; in the middle part of the layer, it is argillic, with spotted dark gray silicification along channels; closer to the top, it is argillic and loose, 0.15–0.3 m thick. The spotted appearance of rock is caused by yellow and reddish yellow pigmentation on segments of the prismatic layer of inocerams shells and oyster valves. In the visible lower part of the layer, an interbed of dark gray carbonate clay (0.3–0.4 m thick) is traced; this interbed is spotted because of breccia-like and lens-like texture: rounded units and fine xenoliths are confined between fine interbeds of dark pelite material. The transition to overlying marls is gradual.

Most of the fossil findings were collected from this and the overlying layer. Thin-walled brachiopod shells (*Gyrosoria lata* (Etheridge), *Orbirhynchia orbignyi* (Pettitt), *Concinnithyris* sp.), large fragments of inoceramus valves (*Cremnoceramus* cf. *waltersdorfensis* (Andert)), and oyster shells are uniformly distributed. There are spines and tests of echinoderms, fragmented and whole skeletons of thin-walled Hexactinnelida sponges (Ventriculitidae), and in the interval between Samples 5/2 and 6/2, a "cluster" of crinoids and starfish is identified. The upper part of the layer is described on the basis of the southern wall of the southernmost trench, whereas the upper one was studied on the basis of cuts made at the base of the northern wall of the middle trench. Owing to a thick deluvial fan, there are two gaps of up to 0.7–1 m in the continuous vertical sequence of the section. Taking the gaps into account, the thickness of the layer is 9.5 m.

Layer 4. Interleaving of light gray dense massive indistinctly laminated marls and a few thin interbeds of argillic cracked marls. Upper beds of massive marls cotain uniformly distributed fine shelly detritus, as well as fragments and fine thin shells of oysters and inoceramids. Fine (3–5 cm thick) beds of light brown pelitic and silty material containing glauconite grains is also identified here. In the middle part of the layer, at the base of massive marls, argillification levels are barely traceable. The base of the layer is assumed to be the one of the lowermost interbed of shelly clayey marl 0.15–0.2 m thick. The thickness of the layer is 15.7–15.8 m.

Layer 5. Interleaving of light gray massive tabular marls and argillic ones of gray color with greenish tone, breccia-like and lens-like texture, containing spherical rounded fragments of dense marls. Interbeds of argillic marls, 0.08–0.1 to 0.4 m thick, are identified in the profile of the wall as niches. At the base (sometimes also at the top) of argillic interbeds, sporadic vertical and diagonal channels filled with white carbonate material can be seen. In massive marls, we traced fine parallel horizontal bedding on argillification levels. The thickness of massive marl interbeds ranges from 0.3–0.4 to 0.5 m. At the base of the layer, marl becomes loose, with relatively large fine fragments of inoceramus valves, whereas a greenish brown pelitic component dominates at its top, emphasizing breccia-like and lens-like texture of rock. The thickness of the layer is 4 m.

Layer 6. The upper and lower intervals of this layer can be distinguished visually. The upper part (about 4.5 m thick) is composed of light gray uniformly colored massive marl with rare lenses of light yellow silty and pelitic marls up to 2–3 cm in size. Dotted and tubular yellow and blackish brown pigmentation is developed. Fragments of inoceramus shells and thin-walled detritus are uniformly distributed and chaotically oriented.

The lower part of the layer is represented by interleaving of dense tabular marls and argillic loose marls containing fine and medium fragments (at the base of this interval, these argillic marls are considered as carbonate breccia-like clays). White massive marls contain scattered and chaotically oriented fragments of thin-walled valves of inoceramids and oysters. The transitions between marl units and between marls and clays are gradual. Clays are dark blue, dark gray, even black in color; spots at the base are produced by variously oriented channels of 0.5–1 cm in diameter filled with dark pelitic material and also by short channels up to 1 mm in diameter. Interbeds of argillic marl or carbonate clays are sometimes characterized by breccia-like texture and gravelly jointing. This is explained by the fact that the bases of these interbeds or the entire interbeds are composed of fine solid rounded units on underlying marls and channels. The surfaces of rounded units sometimes contain signs of bioerosion and selective yellow pigmentation. The thickness of argillic interbed in the middle part of the lower interval (second from the base) is 0.15–0.2 m. At the base of this layer, a bed of carbonate clay of breccia-like and lens-like texture is identified. Here, angular ball-shaped units and rhombus-shaped xenoliths of underlying marls, 2–5 × 5–10 cm in size, occur between irregular lenses of dark gray clays. At the top of this interbed, there are regular and concentrated clay levels, and thin interleaving of marls and clays is seen. The top of argillic marl is clear and steady. Clay interbeds in the lower part of the interval are up to 0.3 m thick. The lower level of argillic marls possessing breccia-like texture coincides with the base of the entire layer. The thickness of the layer is 7.3–7.5 m.

Layer 7. Light gray dense marl containing several interbeds with sponges and mollusks (expressed in the profile of the wall as thin ledges). These levels of clustered fossils are also distinguishable from spotted yellow and reddish yellow staining on skeletons of sponges and molluscan shells. In the lower part of the layer, marl is massive and very dense, with rare skeletons and fragments of subflat thin walls of sponges. Slightly higher, single skeletons of sponges lying on their sides (*Etheridgia* sp., *Paraplocia* sp., Ventriculitidae) are uniformly distributed. The overlying light gray dense marl hosts autochthonously buried sponges *Ortodiscus* sp. and *Becksia* sp. and clusters of horizontally oriented fragments of subflat thin walls of sponges. Above this, marl is massive and dense, containing fragments and deformed skeletons of *Guettardiscyphia roemeri* (Pomel), *G. stellata* (Michelin), *Guettardiscyphia* sp., and *Rhizopoterion* sp. The thickness of the lowermost cluster of sponges is 0.15–0.25 m; transition to the overlying rocks is gradual.

The second sponge-mollusk interbed is represented by fragments of skeletons of sponges (*Plocoscyphia* sp.) appearing in small clusters; it is underlain by gray argillic marl with rare skeletons of *Tremabolites polymorphum* (Sinzov) sponges. We also found large thin inoceramus valves and an echinoderm spine. The third sponge interbed is composed of large subflat fragments of horizontally occurring skeletons (*Ventriculites cribrosus* (Phillips), *Ventriculites* sp., *Ortodiscus* sp.) and chaotically oriented fine fragments of thin inoceramus valves. This third interbed is underlain by marl containing scattered skeletons of thin-walled sponges and gradually transiting downward to looser argillic marl that forms a niche in the profile of the section.

In the upper part of the fourth (counting from bottom) sponge-mollusk interbed, we found an echinoderm spine, inoceramus valves, a brachiopod shell of rinchonelid appearance, and fine oyster valves. The clusters of subautochthonously buried sponges are not regular along the strike, and the level where their skeletons are concentrated (*Guettardiscyphia* sp., *Plocoscyphia* sp., *Zittelispongia* sp.) is located in the upper part of monolithic marl. At 0.1 m below the cluster of sponges and mollusks, a thin interbed of loose argillic marls is identified. At 0.7 m from the top, the uppermost sponge-mollusk interbed is located; it is represented by autochthonously and subautochthonously buried thin-walled (1–3 mm thick) sponges of *Leptophragma murchisoni* (Goldfuss), *Plocoscyphia* sp., *Sporadoscinia* sp., and *Ventriculites* sp. Primary preservation of skeletons is good, while recent preservation is bad because of disintegration of the host rock into rubbly units. The underlying loose marl contains an interval about 1 m thick with uniformly distributed single skeletons of thin-walled sponges of large diameter

(Samples 6–8) and fragments of thin *Pecten* sp. The basal part of the layer is composed of dense indistinctly bedding marl; the base of the layer coincides with the interbed of argillic loose finely broken marl. The entire layer is 8.3–8.5 m thick.

Layer 8. Light green marl, finely bedded in the upper part owing to the lenses and interbeds of pelites and silts, containing fine glauconite grains. Spotted appearance of the rock is caused by pigmentation of channels, skeletons of sponges, and molluscan shells with iron hydroxides. At 0.1 m below the top, an interbed of grayish blue clays 5–7 cm thick is identified; its spotted appearance is caused by silicified channels of dark blue color. Occurring below is an interbed of spotted and sandy marl, with quartz (rarely, glauconite) grains uniformly distributed in it and sometimes forming thin lenses. Marl contains rare phosphorites, black and angular (2–3 cm, rarely up to 5 cm in diameter) or dark brown and well rounded (up to 0.5–1 cm in diameter). Clusters of fine phosphorites and xenoliths of underlying rocks are located at hollows in the erosional surface of the base. The largest inclusions are phosphatized skeletons of sponges (*Paraplocia* sp. and *Ventriculites* sp., more frequently, their fragments), well rounded and carrying traces of bioerosion. Subautochthonously buried skeletons of sponges (*Rhizopoterion* sp. and *Sororistirps* sp.) are filled with silicon earth. The surface of the base is uneven, but can be clearly traced owing to different colors of underlying and overlying rocks and also because of the presence of channels (worm holes) penetrating into the underlying white marl. Holes are filled with light blue siliceous marl containing terrigenous material. Closer to the surface, there are numerous channels 2–3 mm in diameter, whereas below there are rare channels 1–1.5 cm in diameter. The channels are oriented in various directions and can reach depths of 0.05–0.07 to 0.25–0.3 m. The thickness of the layer is 0.1–0.15 m.

Layer 9. Gray clay with greenish tone, spotted because of a nonuniform distribution of light-colored inclusions of silt and carbonates, containing fine fragments. The transition to the overlying marl is gradual. The thickness of the layer is 0.1–0.12 m.

Layer 10. Dense gray marl with greenish tone, nonuniformly spotted because of numerous holes filled with dark blue siliceous cement. The visible thickness of the layer is 0.35–0.4 m.

CHARACERISTICS OF ORYCTOCOMPLEXES AND BIOSTRATIGRAPHY

Belemnites

Belemnites (Figs. 3, 4; Plate I) were collected from the scree in the middle part of the KB-1 section. An incompletely preserved rostrum of *Actinocamax* sp. was defined. Representative specimens of belemnites were taken from the Chukhonastovka-2 section (Fig. 4, Plate I), where *Praeactinocamax triangulus* Naidin and *Praeactinocamax sohzensis* Makhlin were defined; these species characterize lower Turonian rocks of the East European Platform (EEP) (Košťák, 2004; Makhlin, 1973; Naidin, 1964). Worn surfaces of rostra indicate their posthumous short-term transportation.

Bivalves

Inoceramid mollusks (Fig. 4, Plate I) are nonuniformly distributed in the section. Valves appear sporadically, whereas fragments of prismatic layer of shells are uniformly distributed within narrow intervals. Rarely, entire shells of *Cremnoceramus* cf. *waltersdorfensis* (Andert), *C. deformis deformis* (Meek), and *Tethyoceramus* sp. characteristic of the lower Coniacian substage can be found.

It is interesting to discuss the position of the finding identified as *Cremnoceramus* cf. *waltersdorfensis*. In a broader meaning, for the entire species, it is the transitional form of late Turonian–early Coniacian and is known in many regions, e.g., in Western Europe, Mangyshlak, the North Caucasus, the European part of Russia, and, probably, the Caspian Sea region (Aliev and Kharitonov, 1988; Walaszczyk et al., 2004, 2013). The index species of the terminal zone for the upper Turonian is the *C.* cf. *waltersdorfensis waltersdorfensis* subspecies, which is also traced at the base of the lower Coniacian (inoceramus-based deformis erectus Zone). Above, the waltersdorfensis hannovrensis Zone occurs. The studies by I. Walaszczyk showed that the subspecies *waltersdorfensis* and *hannovrensis* are phylogenetically sequential. From this line, at the very beginning of the Coniacian, *C. deformis erectus* (Meek) separates; this species was proposed by Walaszczyk as an index one for the overlying zone (Walaszczyk and Wood, 1998b; Walaszczyk et al., 2010).

The Coniacian GSSP (Global Boundary Stratotype Section and Point) international working group proposed to consider the first appearance of inoceramus species *C. rotundatus* (sensu Troger non Fiege) to be the lower boundary marker of this stratigraphic unit (Kaufman et al., 1996). But revision of the species by Walaszczyk has shown that it is a younger synonym for *C. erectus* (Meek) (Walaszczyk and Wood, 1998b). In this respect, the basal zone of the Coniacian Stage should be named Cremnoceramus deformis erectus, i.e., after the subspecies phylogenetically connected with the *waltersdorfensis–hannovrensis* line. This point was taken into consideration in development of the stratigraphic scheme for Upper Cretaceous deposits of the EEP (Olfer'ev and Alekseev, 2005). Poor preservation of the specimens does not allow us to perform reliable identification up to the subspecies level. Nevertheless, the presence of *waltersdorfensis* suggests that the interval of Samples 71–77 belongs to the boundary between the Turonian and lower Coniacian and is probably included in two sequential zones (deformis erectus and waltersdorfensis hannovrensis).

The subspecies *C. deformis deformis* (Meek) indicates the presence of the terminal inoceramus-based zone of the lower Coniacian (C. crassus crassus/C. deformis deformis) (Walaszczyk and Wood, 1998b). The range of this taxon is widespread, including Western Europe, the Caucasus, the Donets Basin, and the European part of Russia (Dobrov and Pavlova, 1959; Sel'tser et al., 2017; Smirnov and Pergament, 1972). The finding of Tethyoceramus supplements the lower Coniacian complex, because these species are known from the middle and upper parts of the lower Coniacian in the Czech Republic, Germany, Central Asia, the Caspian region, and the North Caucasus (Niebuhr et al., 1999; Walaszczyk and Wood, 1998b).

Brachiopods

Macroscopic brachiopod shells (Figs. 3, 4; Plate I) are rare; most of their findings are located in the middle part of layer 3. Two out of three specimens refer to Terebratulida (*Concinnithyris* sp.) brachiopods, while one refers to Rinchinelida (*Orbirhynchia orbignyi* (Pettitt)) ones. A large number of well-preserved scattered valves of fine brachiopods *Gyrosoria lata* (Etheridge) were found in Sample 5/2 (lower part of layer 3). Fresh cleavage traces on many valves suggest that the shells were separated during maceration. Shell fragments of Cancellothyrididа brachiopods were found in Samples 58, 56, 53, 51, 45, and 2. The significant amount of valves of *Gyrosoria* genus representatives in the middle and upper intervals of layer 8 allowed us to compare carbonate rocks from the KB-1 and Chukhonastovka-2 sections, and a more representative brachiopod complex was distinguished in the latter.

In the Chukhonastovka-2 section, 105 specimens of brachiopods were collected, represented predominantly by entire well-preserved shells with closed valves. The dominating ones are *Gyrosoria lata* (Etheridge) (more than 70%) and *Orbirhynchia* (25%). Among macroscopic species, we determined *Kingena* ex gr. *lima* (Defrance), *Kingena* sp., *Gibbithyris* cf. *semiglobosa* (Sowerby), *Concinnithyris* sp., *Orbirhynchia orbignyi* (Pettitt), and *Orbirhynchia dispansa* Pettitt. Fine brachiopods are represented by *Bisulcina campaniensis* (Orbigny). Inarticulate brachiopods are indicated by a fragment of pedicle valve of *Ancistrocrania* sp.

The brachiopod complexes from the KB-1 and Chukhonastovka-2 sections are characteristic of the Turonian. The *Gyrosoria lata* species is known from the middle and upper Turonian of Western Europe and the lower part of the upper Turonian of the Donets Basin, EEP, Crimea, North Caucasus, Mangyshlak, Cis-Uralian region, Ustyurt, and Kopet Dagh (Kats, 1974; Sklenar and Simon, 2009). The *Orbirhynchia orbignyi* (Pettitt) species is reported in the upper part of the lower Turonian (Mytiloides labiatus Zone) of the Paris Basin (Pettitt, 1954) and in the upper Turonian of the Donets Basin and EEP (Nekhrikova, 1982; Sklenar and Simon, 2009). Representatives of the other groups of brachiopods are transitional.

Echinoderms

Echinoderms (Figs. 3, 4, Plate II) are quite scarce in the KB-1 section. In the upper part of layer 7 (Samples 8 and 12), we found spines of echinoderms, and in the lower part of layer 3 (Samples 79 and 8/2), fragments of *Echinocorys* sp. tests. The study of powders (fraction >0.4 mm) allowed us to trace the distribution of crinoids in particular intervals of this section. Columnals of *Bourgueticrinus* sp. and ?*Nielsenicrinus carinatus* (Roemer) and plates of undeterminable Goniasteridae Forbes, 1841 were recovered from layer 7 (Samples 11–12), layer 5 (Sample 37), layer 4 (Samples 52, 63, and 68–74), and layer 3 (Samples 75–81 and 13/2–5/2) (Fig. 3).

Multiple Echinodermata were recovered from the Chukhonastovka-1 and Chukhonastovka-2 sections. These are mainly crinoids of *Bourgueticrinus* d'Orbigny genus, represented by columnals and stem fragments, by holdfasts of rhizoid type, and also by singular proximals. A single not entire theca, consisting of the proximal part of stem and basal corolla, was assigned to the species *Bourgueticrinus fischeri* (Geinitz), and an isolated proximal was interpreted as one of the species *B. ellipticus* (Miller). Both species are the most ancient representatives of the *Bourgueticrinus* genus and are known from the Turonian (Lach and Salamon, 2016). *B. fischeri* (Geinitz) can be found in the

Plate I. Bivalves and brachiopods from the KB-1 and Chukhonastovka sections. All specimens are shown in their real sizes; magnification is indicated in particular cases. Surfaces of the shown specimens are covered with ammonia chloride. (1) *Cremnoceramus deformis deformis* (Meek), specimen SGU SVB no. 77/1, left valve, KB-1 section, uppermost layer 4–lowermost layer 6, lower Coniacian; (2) *Cremnoceramus* cf. *waltersdorfensis* (Andert), specimen SGU SVB no. 77/2, left valve, KB-1 section, uppermost layer 3–lower part of layer 4; (3) *Tethyoceramus* sp., specimen SGU SVB no. 77/4, left valve, KB-1 section, lowermost layer 4–layer 5, lower Coniacian; (4) *Praeactinocamax triangulus* Naidin, specimen SGU SVB no. 77/5, incomplete rostrum (4a, view from alveolus side (×3); 4b, dorsal view; 4c, side view), Chukhonastovka-1 section, layer 3, (?) lower Turonian; (5) *Praeactinocamax sohzensis* Makhlin, specimen SGU SVB no. 77/8 (5a, dorsal view; 5b, side view), Chukhonastovka-1 section, layer 3, (?) lower Turonian; (6) *Orbirhynchia orbignyi* (Pettitt) with attached *Serpulidae* s.l., specimen SGU no. 251/13-01 (6a, pedicle valve; 6b, brachial valve; 6c, side view; 6d, view on the frontal margin (×2)), KB-1 section, middle part of layer 3, upper Turonian; (7) *Gyrosoria lata* (Etheridge), specimen SGU no. 251/12-22 (7a, pedicle valve; 7b, brachial valve; 7c, side view; 7d, view on the frontal margin (×4)), KB-1 section, layer 3, upper Turonian; (8) *Kingena* ex gr. *lima* (Defrance), specimen SGU no. 251/12-03 (8a, pedicle valve; 8b, brachial valve; 8c, side view; 8d, view on the frontal margin (×2)), Chukhonastovka-2 section, layer 6, middle Turonian.

Plate I

Turonian–Santonian deposits of Western Europe, Crimea, Mangyshlak, and Turkmenistan (Klikushin, 1980, 1982; Lach and Salamon, 2016). Beyond the limits of the discussed region, *B. ellipticus* (Miller) is reported in the lower Turonian–upper Campanian of Belgium, the Czech Republic, England, Germany, France, Sweden, Poland, and Ukraine. Rarer columnals and stem fragments belong to crinoids of *Pentacrinites*. Turonian *Pentacrinites* on the EEP are represented by singular columnals of two species, "*Pentacrinites*" *exilis* and *Isocrinus*? [=*Nielsenicrinus*] *carinatus*, from chalkstone deposits of Ternopil oblast, Ukraine (Klikushin, 1991). Columnals of *Pentacrinites* from the Volga region are rounded-pentagonal in shape, with the characteristic spine-like ornaments based on whose morphology they can be assigned to *Nielsenicrinus carinatus* (Roemer), the species known in the Coniacian–Campanian deposits of northern part of Western Europe, Ukraine, Kazakhstan, Turkmenistan, and Crimea.

Echinoderms are represented by multiple spine fragments, pieces of *Echinocorys* sp. tests, and individual plates of Cidaridae Gray. The interesting finding is *Gauthieria radiata* (Sorignet), the first and the only one in the Volga region. This species is reported in Turonian–Santonian deposits (Mytiloides labiatus–Micraster coranguinum zones) of Algeria, Western and Eastern Europe, Western Ukraine, and the Donets Basin (Smith and Wright, 1996).

Starfish are represented by multiple marginal plates of Goniasteridae Forbes, while only a fragment of *Ophiotitanos serrata* (Roemer) arm represents brittle stars. Note that this species is common in Late Cretaceous–Paleogene deposits of Great Britain, Germany, the Czech Republic, Netherlands, Belgium, France, Denmark, Sweden, and also, probably, Poland, Spain, the United States, and Tunisia (Storc and Zitt, 2008).

Spongiofauna

In the KB-1 section, several levels with Hexactinnelida sponges were revealed; spiculas of siliceous sponges were noticed in microfaunal samples (Figs. 3, 4).

The first level where skeletons of sponges concentrated is the interval of the middle Cenomanian–middle Turonian. In the KB-1, KB-2, Chukhonastovka-1, Melovatka-9, and Krasnyi Yar-1 sections, the taxonomy of the Cenomanian spongiocomplex is more diverse compared to the Turonian one, and the amount of representatives is also greater. Cenomanian sands and silts contain abundant skeletons of tiny and thin-walled Hexactinnelida *Balantionella* (B.) *melovatkensis* Perv., *Camerospongia ilovlensis* Perv., *Guettardiscyphia trilobata* (Roemer), *G. stellata* (Michelin), *Etheridgia* sp., *Paraplocia* sp., *Paracraticularia* sp., and Ventriculitidae, and, less commonly, Demospongiae, rounded and phosphatized to different degrees (Pervushov, 2016a, 2016b, 2018). Sponges from the Turonian oryctocomplex differ in weak phosphatization, larger sizes, thicker walls, and carbonate filling of the inner space; the fossils (including sponges) redeposited from Cenomanian rocks are common in this complex.

The second level was distinguished in Middle Coniacian marls (layer 7). Earlier, the presence of yellow-colored (because of iron hydroxides) sponges in the upper intervals of Turonian–Coniacian was reported in near-Khoper area (Semenov, 1959). Given that a few specimens can be defined within species accuracy because of the degree of preservation, the Coniacian sponge assemblage is identical in taxonomy to the spongiocomplex from the lower Santonian "sponge" horizon. Intervals of Middle Coniacian marls in the KB-1, Melovatka, Krasnyi Yar, and Splavnukha-2 sections demonstrate a gradual increase in amount and diversity of sponges and density of their communities; this is attributed to regressive tendencies

Plate II. Echinoderms and radiolarians from the KB-1 and Chukhonastovka-2 sections. (1) *Ophiotitanos serrata* (Roemer), specimen PIN no. 5625/1, arm fragment (1a, view from top; 1b, view from bottom; 1c, lateral view), Chukhonastovka-2 section, layer 6, middle–upper Turonian; (2) *Bourgueticrinus fischeri* (Geinitz), specimen PIN no. 5625/2, proximal part of stem with basal corolla (2a, lateral view; 2b, lateral view from top), Chukhonastovka-2 section, layer 6, middle–upper Turonian; (3) *Bourgueticrinus ellipticus* (Miller), specimen PIN no. 5625/3, proximal (3a, lateral view; 3b, lateral view from bottom), Chukhonastovka-2 section, layer 6, middle–upper Turonian; (4) *Bourgueticrinus* sp., specimen PIN no. 5625/4, articulation surface of columnal stem, Chukhonastovka-2 section, layer 6, middle–upper Turonian; (5) *Bourgueticrinus* sp., specimen PIN no. 5625/5, columnal stem, lateral view, Chukhonastovka-2 section, layer 6, middle–upper Turonian; (6) *Bourgueticrinus* sp., specimen PIN no. 5625/6, columnal stem (6a, articulation surface, view from top; 6b, lateral view from top), Chukhonastovka-2 section, layer 6, middle–upper Turonian; (7) *Bourgueticrinus* sp., specimen PIN no. 5625/7, holdfast fragment (7a, lateral view; 7b, lateral view from top; 7c, view from top), Chukhonastovka-2 section, layer 6, middle–upper Turonian; (8) *Nielsenicrinus carinatus* (Roemer), specimen PIN no. 5625/8, articulation surface of columnal, Chukhonastovka-2 section, layer 6, middle–upper Turonian; (9) *Nielsenicrinus carinatus* (Roemer), specimen PIN no. 5625/9, stem fragment (9a, lateral view; 9b, lateral view from top), Chukhonastovka-2 section, layer 6, middle–upper Turonian; 10, Goniasteridae gen. et sp. indet., specimen PIN no. 5625/10, marginal plate, Chukhonastovka-2 section, layer 6, middle–upper Turonian; (11) Goniasteridae gen. et sp. indet., specimen PIN no. 5625/11, marginal plate (11a, articulation surface, view from top; 11b, lateral view from top), Chukhonastovka-2 section, layer 6, middle–upper Turonian; (12) Goniasteridae gen. et sp. indet., specimen PIN no. 5625/12, marginal plate (12a, lateral view; 12b, lateral view from top), Chukhonastovka-2 section, layer 6, middle–upper Turonian; (13) *Gauthieria radiata* (Sorignet), specimen SGU no. 206/6 (13a, view from top; 13b, view from bottom; 13c, lateral view), Chukhonastovka-2 section, layer 6, middle–upper Turonian; (14) *Dictyomitra formosa* Squinabol, specimen SGU no. 260/BK-1-02, KB-1 section, layer 2, lower Santonian; (15) *Orbiculiforma* cf. *maxima* Pessagno, specimen SGU no. 260/BK-1-02, KB-1 section, layer 2, lower Santonian; (16) *Crucella aster* (Lipman), specimen SGU no. 260/BK-1-02, KB-1 section, layer 2, lower Santonian. Lengths of scale bars are 500 μm (3, 8), 1000 μm (1, 2, 4–7, 9–12), 1 cm (13), and 100 μm (14–16).

Plate II

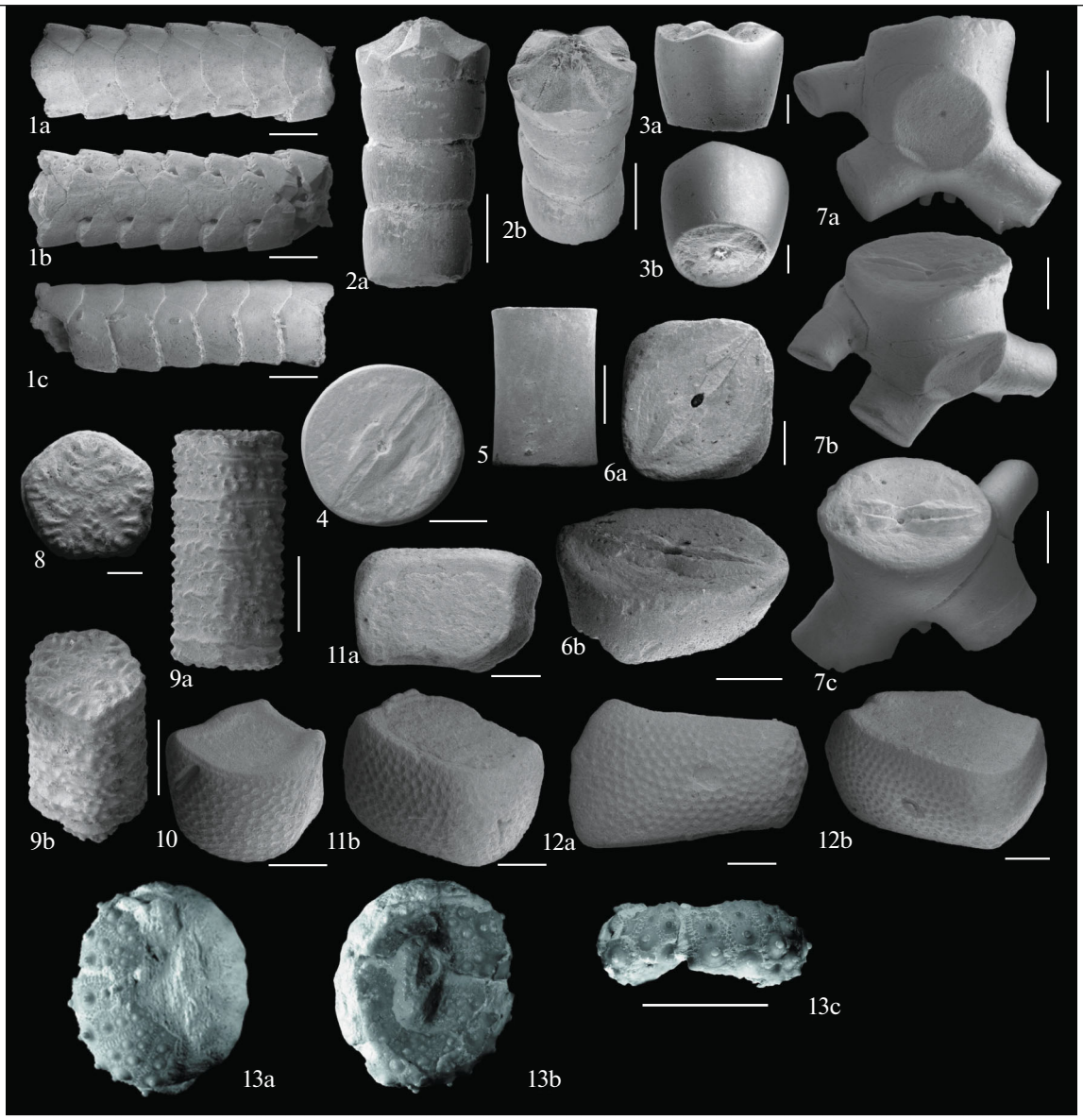
1a
1b
1c
2a
2b
3a
3b
4
5
6a
6b
7a
7b
7c
8
9a
9b
10
11a
11b
12a
12b
13a
13b
13c

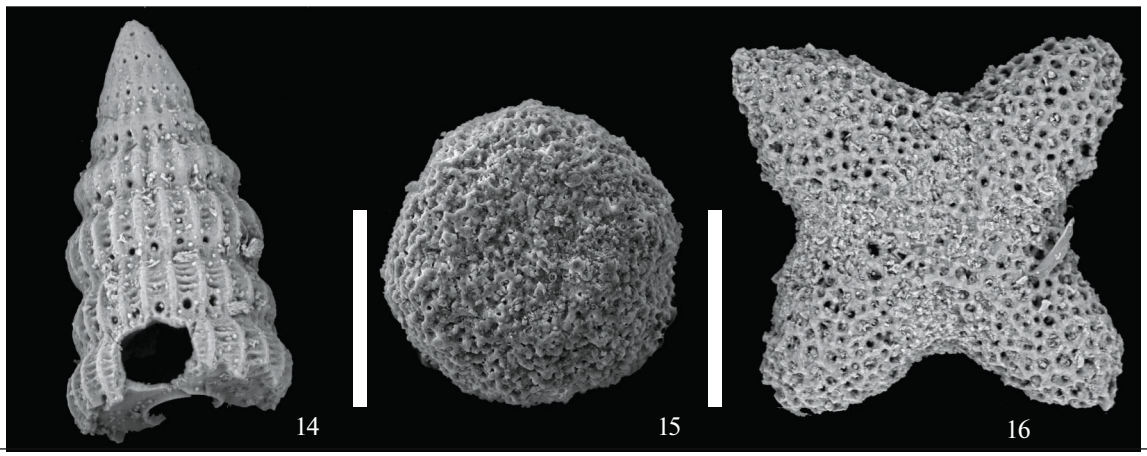
14
15
16

of the basin evolution. Settlement of sponges in the middle Turonian–early Coniacian was associated with northward advance of the marine basin along submeridional depressions. The distribution of sponges was predetermined by peculiarities of currents within the basin, which promoted the appearance of communities of sponges remaining as interbeds containing subautochthonously and synchronously buried skeletons of sponges. In the greater part of the region, Coniacian (sometimes also Turonian) rocks are washed out; therefore, reliable data on the Coniacian spongiocomplex were not available. Washing out of Turonian–Coniacian carbonate rocks led to the fact that some destruction-proof fossils were redeposited to the base of the lower Santonian "sponge" horizon.

The third level where sponges are abundant is the lower Santonian "sponge" horizon which is widespread on the EEP (Pervushov, 2016b). In the KB-1 section, it points out the surface of stratigraphic unconformity and change in lithology of rocks. The phosphorite horizon with fragments of sponges is thin. Skeletons are highly phosphatized, often appearing as pebbles pierced by multiple holes of lithophages. At the late stages of succession of sponges, the species settled in the region were those preferring quiet conditions of laminar flows of near-bottom waters. Skeletons of these species are subautochthonously buried and filled with silicon earth (*Sororistirps* sp., *Rhizopoterion* sp.). In the middle Coniacian and early Santonian spongiocomplexes, only transitional species (*Guettardiscyphia*, *Etheridgia*, Plocoscyphia, and *Tremabolites*) were revealed.

Benthic Foraminifera

Benthic foraminifera (BF; Figs. 5, 6; Plates III–V), as well as planktonic ones, have been found in all samples but in different quantitative relationships (Fig. 5). Distinguishing of BF zones was made on the basis of the infrazonal scheme of the Upper Cretaceous subdivision for the EEP (Beniamovsky, 2008a, 2008b), taking into account the recent corrections introduced by V.N. Beniamovsky (Vishnevskaya et al., 2018). The ranks of taxa were based on the classification by Loeblich and Tappan (1988), taking into account the restored genus *Pseudovalvulineria* Brotzen, 1942, which was used for the phylogenetic series *Pseudovalvulineria kelleri kelleri–P. stelligera* and *P. praeinfrasantonica–P. vombensis* and also the *P. thalmanni* (Brotzen) and *P. lorneiana* (d'Orbigny) species (Vasilenko, 1954). For the *Stensioeina* genus (Dubicka and Peryt, 2014), two subgenera were distinguished (*Protostensioeina* and *Stensioeina*), and this was also reflected in the names of zones and subzones.

In the KB-1 section, we distinguished five BF-based foraminiferal zones (Fig. 5). At the base of the section (layer 1), near the condensed interbed, we revealed the mixed complex including the species characteristic of both the Cenomanian and lower–middle Turonian. Their shells are fine and poorly preserved; the determined taxa include *Globorotalites multiseptus* Brotzen, *Pseudovalvulineria vesca* (Bykova), *P.* cf. *nana* (Akimetz), *Gavelinella* cf. *polessica* (Akimetz), *Gyroidinoides nitidus* (Reuss), and *Cibicides pollyrraphes pollyrraphes* (Reuss).

Up the section, the complex of the middle Turonian Gavelinella moniliformis moniliformis/G. ammonoides (LC4) Zone was identified, with two subzones within its limits. The lower one, Gavelinella ammonoides/Marssonella oxycona (LC4a), is characterized by the presence of both agglutinating taxa—*Tritaxia tricarinata* (Reuss), *T. cenomana* Gorbenko, *Marssonella oxycona* (Reuss), *M. conulus* (Reuss), *Eggerelina brevis* (d'Orbigny), *Arenobulimina presli* (Reuss), and *Gaudryina arenosa* Akimetz—and secreting ones—*Eponides carsteni* (Reuss), *E. belorusiensis* Akimetz, *Valvulineria lenticula* (Reuss), *Gyroidinoides nitidus* (Reuss), *Globorotalites multiseptus* Brotzen., *Gavelinella ammonoides* (Reuss), *G. moniliformis moniliformis* (Reuss), *Pseudovalvulineria vesca* (Bykova), *Cibicidoides gorbenkoi* (Akimetz), *Cibicides pollyrraphes pollyrraphes* (Reuss), *Praebulimina reussi* (Morrow), *Eouvigerina regularis* (Keller), *Tappanina eouvigeriniformis* (Keller), *T. selmensis* (Cushman), and *Reussella carinata* Vasilenko.

Plate III. Benthic foraminifera (BF) from the KB-1 section. (1) *Protostensioeina pokornyi* (Scheibnerova), specimen SGU no. 260/BK-2-07, layer 3, middle–upper Turonian; (2) *Stensioeina praeexculpta* (Keller) [*Protostensioeina* sp. E Dubicka et Peryt], specimen SGU no. 260/BK-2-13, layer 3, middle–upper Turonian; (3) *Tappanina eouvigeriniformis* (Cushm.), specimen SGU no. 260/BK-2-03, layer 2, middle–upper Turonian; (4) *Protostensioeina polonica* (Witwicka) [=*St. laevigata* Akim.], specimen SGU no. 260/BK-2-13, layer 3, middle–upper Turonian; (5) *Protostensioeina granulata* (Olbertz), specimen SGU no. 260/BK-1-77, layer 3, middle–upper Turonian; (6) *Protostensioeina bohemica* (Jirova), specimen SGU no. 260/BK-1-45, layer 4, lower Coniacian; (7) *Protostensioeina* sp., specimen SGU no. 260/BK-1-47, layer 4, lower Coniacian; (8) *Marssonella conulus* (Reuss), specimen SGU no. 260/BK-1-45, layer 4, lower Coniacian; (9) *Marssonella oxycona* (Reuss), specimen SGU no. 260/BK-1-77, layer 3, middle–upper Turonian; (10) *Verneuilina muenstery* Reuss, specimen SGU no. 260/BK-1-77, layer 3, middle–upper Turonian; (11) *Reussella carinata* Vass., specimen SGU no. 260/BK-2-03, layer 2, middle–upper Turonian; (12) *Reussella* trans. from *carinata* to *kelleri* Vasilenko, specimen SGU no. 260/BK-1-77, layer 3, middle–upper Turonian; (13) *Reussella kelleri* Vass., specimen SGU no. 260/BK-1-29, layer 6, middle Coniacian; (14) *Protostensioeina granulata incondita* Koch., specimen SGU no. 260/BK-1-43, base of layer 5, lower Coniacian; (15) *Eouvigerina cretacea* (Cushm.), specimen SGU no. 260/BK-1-45, top of layer 4, lower Coniacian; (16) *Protostenioeina granulata perfecta* Koch, specimen SGU no. 260/BK-1-22, layer 6, middle Coniacian; (17) *Protostensioeina* sp. A Dubicka et Peryt [=*Stensioeina emscherica* Baryschn.], specimen SGU no. 260/BK-1-30, base of layer 6, middle Coniacian; (18) *Protostensioeina granulata incondita* (Koch), specimen SGU no. 260/BK-1-18, layer 7, middle Coniacian. Letter indices at numbers of images denote (a) view from dorsal side, (b) view from ventral side, and (c) view from aperture side. Scale bar is 100 μm.

Plate III

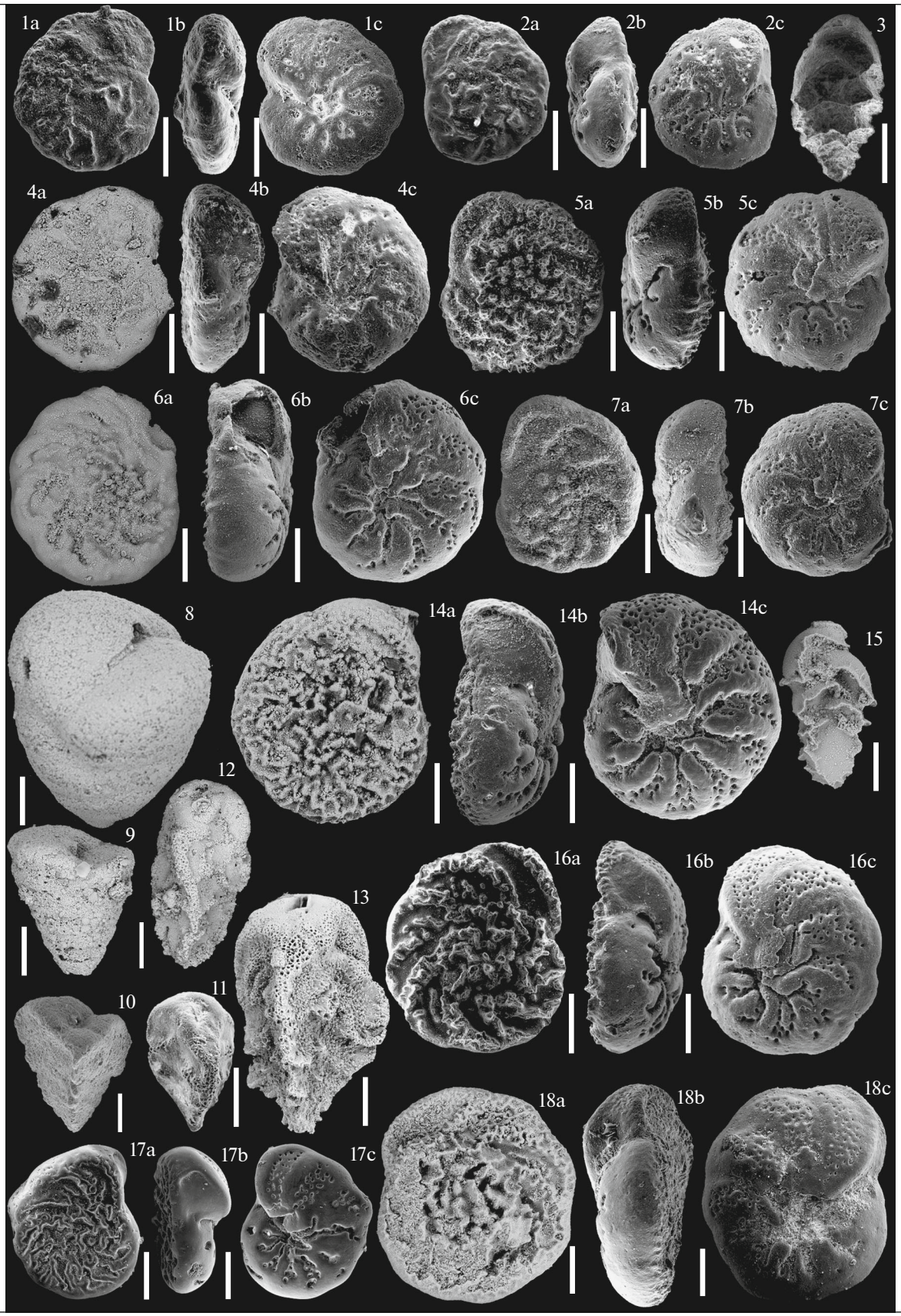
1a
1b
1c
2a
2b
2c
3
4a
4b
4c
5a
5b
5c
6a
6b
6c
7a
7b
7c
8
14a
14b
14c
15
12
9
16a
16b
16c
13
10
11
18a
18b
18c
17a
17b
17c

The upper subzone, Gavelinella moniliformis ukrainica (LC4b), is distinguished from the appearance of an index species and a number of new taxa: *Lituolla irregularis* (Roemer), *Gaudryina laevigata* Franke, *G. folium* Akimetz, *Berthelina berthelini* (Keller), *Cibicides polyrraphes juncta* Vasilenko. The BF complex of the middle Turonian LC4 Zone is close to that of the Gavelinella ammonoides Zone identified within the upper Turonian (at a two-unit subdivision) of the Polesye saddle and some other sections of the EEP (Akimets, 1981; Olfer'ev et al., 2007; Walaszczyk et al., 2004).

In the middle and upper parts of layer 3, we identified the Stensioeina praeexculpta/Ataxophragmium compactum (LC5) Zone represented in the KB-1 section by the Protostensioeina praeexculpta (LC5a) Subzone of the middle–upper Turonian.

In the LC5a complex, we revealed all taxa from the underlying zone, excluding representatives of *Gavelinella ammonoides*, which were found only in Sample 7/2 (argillic interbed) within this interval. The development of *Stensioeina* genus representatives also begins from this interval. Beginning from the base of this zone, such taxa as *Ataxophragmium initiale* Woloschina, *Verneuilina muensteri* Reuss, *Spiroplectamina praelonga* (Reuss), *Eggerelina sphaerica* (Reuss), *Heterostomella carinata* (Franke), *Marssonella conulus* (Reuss), *Planularia complanata* (Reuss), *Frondicularia* sp., *Protostensioeina pokornyi* (Scheibnerova), *Protostensioeina* sp. E Dubicka et Peryt [=*Stensioeina praeexculpta* (Keller)], and *Cibicidoides praeeriksdalensis* (Vasilenko) appear. In the middle part of the zone, we identified *Osangularia dorsoconvexa* (Woloschina) and *Protostensioeina polonica* (Witwicka) [=*Stensioeina laevigata* Akimetz]. In the upper part of the zone, single *Osangularia whitei whitei* (Brotzen.), *Protostensioeina granulata* (d'Orbigny), and *Pseudovalvulineria kellery* (Mjatluk) *dorsoconvexa* (Akimetz) appear, as well as transitional forms from *Reussella carinata* Vasilenko to *R. kelleri* Vasilenko. Note that the species *Protostensioeina pokornyi* (Scheibnerova) was identified within the limits of the EEP for the first time; it is characteristic of the lower–middle Turonian of the northwestern part of Germany (Koch, 1977), where the level of its appearance correlates to the level of *Inoceramus labiatus* Schlotheim. The complex is characteristic of the EEP and similar to the upper Turonian (at a two-unit subdivision) complexes of the Volyn-Podolsk Plate, Dnieper-Donets Basin, Poland, Sweden, and, partially, Mangyshlak (Vasilenko, 1961).

The KB-1 section does not include the Ataxophragmium compactum (LC5b) and Reussella kelleri (LC5c) subzones, to which the beginning of the "Ataxofragmium" and "Reussella" evolution stages of Late Cretaceous BF is related (Beniamovsky, 2008a). This indicates the presence of a hiatus between the middle–upper Turonian and lower Coniacian deposits. The duration of this interval can be estimated at 720 k.y. (Vishnevskaya et al., 2018).

The complex revealed in layers 4, 5, and 6 (lowermost) is characteristic of the Protostensioeina emscherica/P. granulata (LC6a) Subzone of the lower Coniacian Protostensioeina emscherica/Pseudovalvulineria kelleri kelleri (LC6) Zone.

The lower boundary of the LC6 Zone is drawn according to the first appearance of the index species *Pseudovalvulineria kelleri kelleri* (Mjatluk). The characteristic feature is constant presence of the *Protostensioeina granulata* (d'Orbigny) species and its varieties, *Protostensioeina* sp. B (Dubicka et Peryt) and *P.* sp. D (Dubicka et Peryt), which, judging by the earlier data, was determined as *Stensioeina emscherica* Baryschnikova (Baryshnikova, 1959; Sadekov and Benyamovsky, 2009), one of the index species of this zone. The complex is renewed owing to such agglutinating species as *Ataxophragmium compactum* Brotzen., *At. nautiloides* (Brotzen.), *Arenobulimina frons* Olszewski, and *Spiroplectaminna embaensis* (Mjatluk) and secreting ones—*Planularia decora* Lipnik, *Robulus* sp., *Lenticulina secans* (Reuss), *Palmula baudouiniana* (d'Orbigny), *Eponides concinnus* Brotzen., *Pseudovalvulineria praeinfrasantonica* (Mjatluk), *Gavelinella tumida* Brotzen., *Reussella kelleri* Vasilenko, and *Eouvigerina cretacea* (Cushman). At the base of layer 4, representatives of *Gaudryina arenosa* Akimetz, *Berthelina berthelini* (Keller), and *Tappanina* genus are not

Plate IV. BF from the KB-1 section. (1) *Pseudovalvulineria vesca* (Byk.), specimen SGU no. 260/BK-2-03, layer 2, middle–upper Turonian; (2) *Gavelinella ammonoides* (Reuss), specimen SGU no. 260/BK-1-45, layer 4, lower Coniacian; (3) *Ataxophragmium compactum* Brotz., specimen SGU no. 260/BK-1-74, base of layer 4, lower Coniacian; (4) *Pseudovalvulineria praeinfrasantonica* (Mjatl.), specimen SGU no. 260/BK-1-05, top of layer 7, middle Coniacian; (5) *Gavelinella moniliformis ukrainica* (Vass.), specimen SGU no. 260/BK-2-05, layer 3, middle–upper Turonian; (6) *Praebulimina reussi* (Morrow), specimen SGU no. 260/BK-2-12, layer 3, middle–upper Turonian; (7) *Pseudovalvulineria kelleri kelleri* (Mjatl.), specimen SGU no. 260/BK-1-74, base of layer 4, lower Coniacian; (8) *Gavelinella tumida* Brotz., specimen SGU no. 260/BK-1-46, layer 4, lower Coniacian; (9) *Pseudovalvulineria* aff. *lorneiana* (d'Orb.), specimen SGU no. 260/BK-1-61, layer 4, lower Coniacian; (10) *Pseudovalvulineria thalmanni* (Brotz.), specimen SGU no. 260/BK-1-27, layer 6, middle Coniacian; (11) *Gavelinella pertusa* (Marss.), specimen SGU no. 260/BK-1-24, layer 6, middle Coniacian; (12) *Gavelinella costulata* (Marie), specimen SGU no. 260/BK-1-31, lower part of layer 6, lower Coniacian; (13) *Gavelinella umbilicatula* (Mjatl.), specimen SGU no. 260/BK-1-05, layer 7, middle Coniacian; (14) *Pseudovalvulineria vombensis* Brotz., specimen SGU no. 260/BK-1-02, layer 9, lower Santonian; (15) *Cibicidoides praeeriksdalensis* (Vass.), specimen SGU no. 260/BK-1-06, layer 7, middle Coniacian; (16) *Cibicidoides eriksdalensis* (Brotz.), specimen SGU no. 260/BK-1-02, layer 9, lower Santonian; (17) *Ataxophragmium crassum* (d'Orb.), specimen SGU no. 260/BK-1-07, layer 7, middle Coniacian. Letter indices at numbers of images denote (a) view from dorsal side, (b) view from ventral side, and (c) view from aperture side. Scale bar is 100 μm.

Plate IV

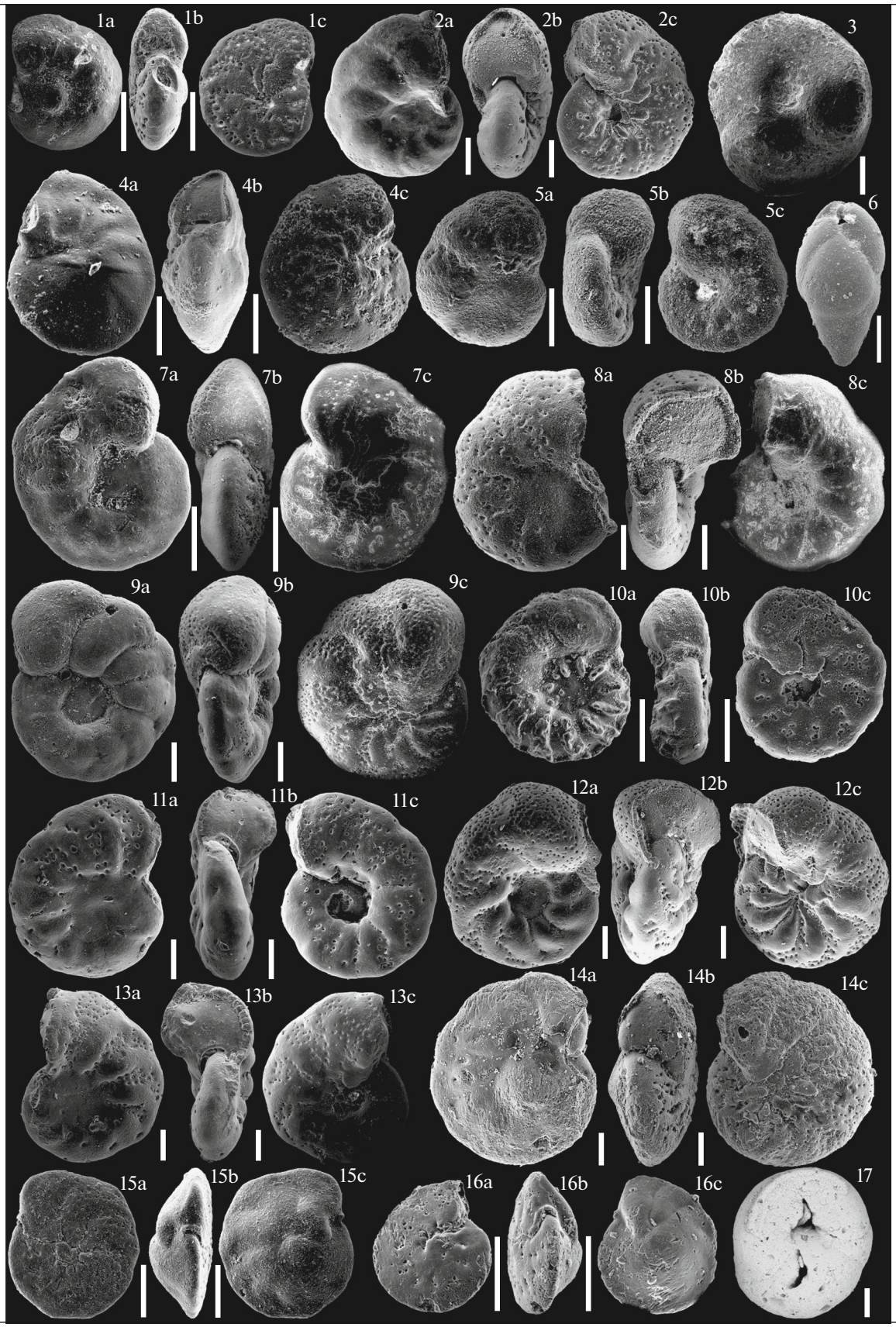
1a
1b
1c
2a
2b
2c
3
4a
4b
4c
5a
5b
5c
6
7a
7b
7c
8a
8b
8c
9a
9b
9c
10a
10b
10c
11a
11b
11c
12a
12b
12c
13a
13b
13c
14a
14b
14c
15a
15b
15c
16a
16b
16c
17

encountered. Upon approaching the top of layer 5, such species as *Marssonella oxycona* (Reuss), *M. conulus* (Reuss), *Cibicides pollyrraphes juncta* Vasilenko, *Gavelinella moniliformis ukrainica* (Vasilenko), and *Pseudovalvulineria kellery* (Mjatlyuk) *dorsoconvexa* (Akimetz) gradually disappear.

In this interval, we revealed a number of bioevents related to the appearance of stratigraphically important taxa. In Sample 67, representatives of *Protostensioeina* sp. B Dubicka et Peryt [=*Stensioeina emscherica* Baryschnikova] appear; in Sample 62, *P.* sp. D Dubicka et Peryt [=*Stensioeina laevigata* (Akimetz]) and *Pseudovalvulineria* aff. *lorneiana* (d'Orbigny) appear. Beginning from Sample 57, *Gavelinella ammonoides* (Reuss) reappears; it is the ancestral species of Coniacian *Gavelinella costulata* (Marie) identified higher in the section, in layer 5 (beginning from Sample 31). Starting from the base of layer 5 (Sample 43), *Protostensioeina bohemica* (Jirova) and *P. granulata* incondita (Koch) appear, and in the base of layer 6, we found *Osangularia whitei praeceps* (Brotzen).

In Sample 30 we identified the first appearance of the *Pseudovalvulineria thalmanni* (Brotzen.) species, giving grounds to distinguish here the Pseudovalvulineria thalmanni (LC7) Zone of the middle Coniacian. The complex is considerably renewed owing to the appearance of a number of secreting taxa: *Protostensioeina granulata perfecta* (Koch), *P.* sp. A Dubicka et Peryt, *Globorotalites mischelianius* (d'Orbigny), *Gyroidinoides turgidus obliquseptatus* (Mjatluk), and *Pseudovalvulineria thalmanni* (Brotzen.), as well as single *P. vombensis* Brotzen., *Gavelinella costulata* (Marie), *G. umbilicatula* (Mjatluk), *G. pertusa* (Marsson), and *Praebulimina carsaye* (Plummer). At the base of layer 7, *Eouvigerina cretacea* (Cushman) disappears and the first appearance of the *Neoflabelina* genus is reported. In layers 7–10, we determined *Neoflabelina suturalis suturalis* (Cushman), *N. gibbera* (Wedekind), and *N.* cf. *suturalis suturalis* (Cushman), as well as single agglutinating *Ataxophragmium crassum* (d'Orbigny) and *Gaudryina rugosa* (d'Orbigny).

Above the "sponge" horizon, in the interbed of silicified clay, we found the complex characteristic of the early Santonian Cibicidoides eriksdalensis (LC8c) Subzone of the Stensioeina exculpta exculpta (LC8) Zone. The complex is represented by taxa commonly distributed below: *Arenobulimina carseyae* Olszew, *Novatrix obesa* (Reuss), *Globorotalites mischelianius* (d'Orbigny), *Osangularia whitei whitei* (Brotzen), *Gavelinella* cf. *tumida* Brotzen; it is renewed by the appearance of *Spiroloculina cretacea* Reuss, *Cibicidoides eriksdalensis* (Brotzen), *Cibicides excavatus* Brotzen, and *Loxostomum eleyi* (Cushman), typical of the lower Santonian Pseudovalvulineria vombensis Brotzen Zone. We also found large Nodozariida.

Planktonic Foraminifera

Planktonic foraminifera (PF) (Figs. 5, 7; Plate VI) are represented by two groups: spirally conic shells of globotruncanids and spirally screw shells of heterohelicids. Spirally planar foraminifera of the planomalinids have not been found.

The spirally conic globotruncanids are in their absolute majority represented by taxa characterized by primitive structure of shells: chambers are without complex ornamentation, and extraumbilical aperture is simple. These are species of the *Whiteinella* and *Archaeoglobigerina* genera. The first representatives of the *Whiteinella* genus are found in Sample 3/2 and can be seen throughout the entire section. These are species *W. archaeocretacea* Pessagno and *W. aumalensis* (Sigal). The distribution of *W. aumalensis* species is limited to the Cenomanian–Turonian deposits, whereas *W. archaeocretacea* can be found in in the interval from the upper Cenomanian to Santonian inclusively. In Sample 5/2, the *W. paradubia* (Sigal) and *W. baltica* Douglas et Rankin species appear. According to the ideas of some authors, the distribution of *W. paradubia* species is limited to the Turonian and Coniacian (Caron, 1985), although other researchers believe it to be more widespread (Walaszczyk and Peryt, 1998a). The *W. baltica* species can be found from the upper Cenomanian to lower Campanian inclusively. The taxa with keeled peripheral rim and wider aperture are represented in the lower part of the section by two species of the *Dicarinella* genus: *D. imbricata* (Mornod) and *D.* cf. *algeriana* Caron. Findings of these shells are

Plate V. BF from the KB-1 section. (1) *Cibicides pollyrraphes pollyrraphes* (Reuss), specimen SGU no. 260/BK-2-01, layer 1, Cenomanian; (2) *Cibicides pollyrraphes juncta* Vass., specimen SGU no. 260/BK-2-11, layer 3, middle–upper Turonian; (3) *Cibicides excavates* Brotz., specimen SGU no. 260/BK-1-02, layer 9, lower Santonian; (4) *Osangularia dorsoconvexa* Wolosch., specimen SGU no. 260/BK-2-12, layer 3, middle–upper Turonian; (5) *Osangularia whitei whitei* (Brotz.), specimen SGU no. 260/BK-1-75, top of layer 3, middle–upper Turonian; (6) *Osangularia whitei praeceps* (Brotz.), specimen SGU no. 260/BK-1-37, layer 5, lower Coniacian; (7) *Osangularia whitei* spp., specimen SGU no. 260/BK-1-01, layer 10, lower Santonian; (8) *Gaudryina arenosa* Akim., specimen SGU no. 260/BK-2-09, layer 3, middle–upper Turonian; (9) *Gaudryina folium* Akim., specimen SGU no. 260/BK-1-74, base of layer 4, lower Coniacian; (10) *Gaudryina laevigata* Franke, specimen SGU no. 260/BK-2-05, layer 3, middle–upper Turonian; (11) *Eggerelina brevis* (d'Orb.), specimen SGU no. 260/BK-2-13, layer 3, middle Turonian; (12) *Novatrix obesa* (Reuss), specimen SGU no. 260/BK-1-02, layer 9, lower Santonian; (13) *Heterostomella carinata* Franke, specimen SGU no. 260/BK-1-17, layer 7, middle Coniacian; (14) *Neoflabelina gibbera* (Wed.), specimen SGU no. 260/BK-1-16, layer 7, middle Coniacian; (15) *Neoflabelina* cf. *gibbera* (Wed.), specimen SGU no. 260/BK-1-02, layer 9, lower Santonian; (16) *Ataxophragmium* aff. *compactum* Brotz., specimen SGU no. 260/BK-1-27, layer 6, middle Coniacian; (17) *Loxostomum eleyi* (Cushm.), specimen SGU no. 260/BK-1-02, layer 9, lower Santonian. Letter indices at numbers of images denote (a) view from dorsal side, (b) view from ventral side, and (c) view from aperture side. Scale bar is 100 μm.

Plate V

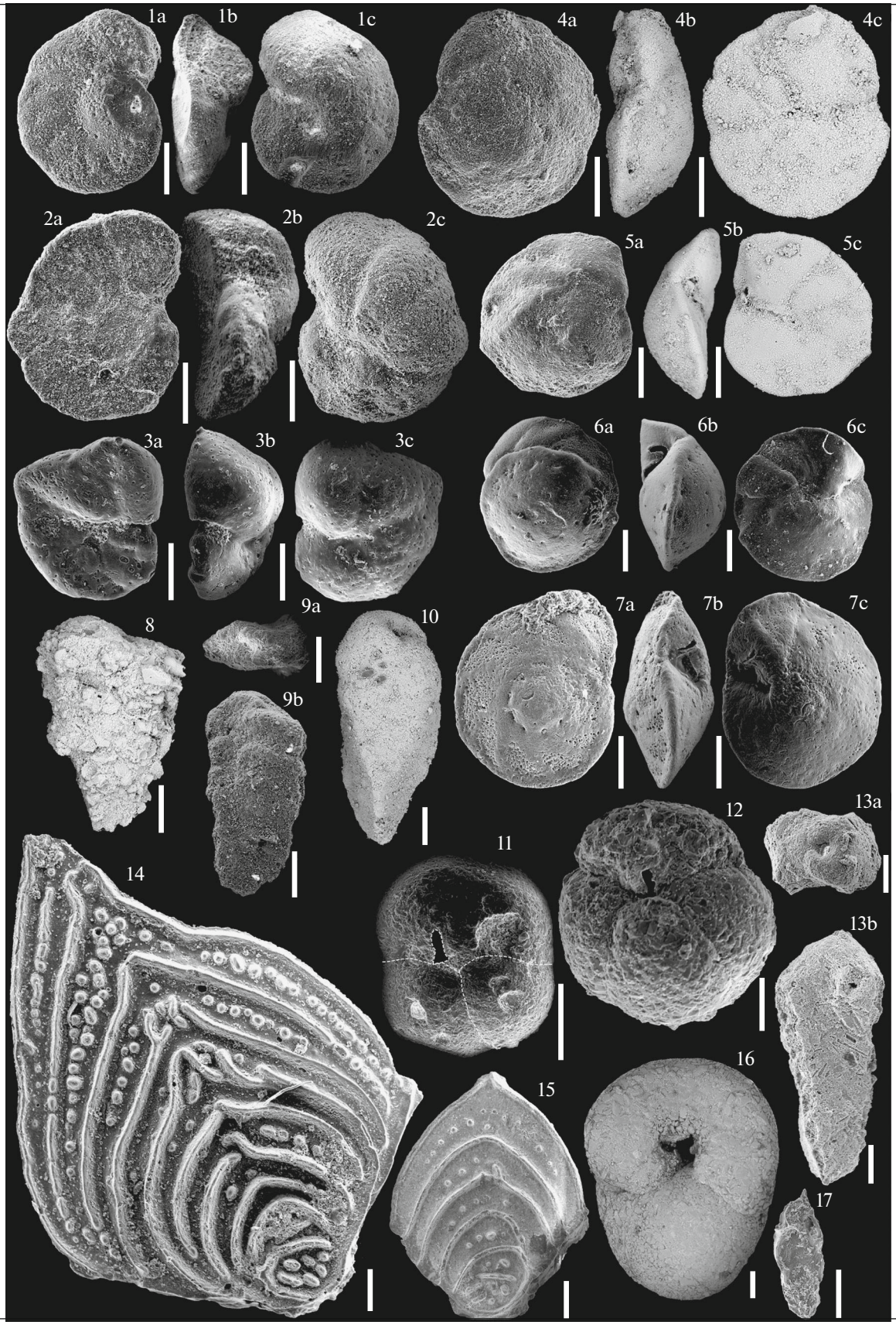
1a
1b
1c
4a
4b
4c
2a
2b
2c
5a
5b
5c
3a
3b
3c
6a
6b
6c
8
9a
10
7a
7b
7c
9b
12
13a
14
11
13b
16
15
17

singular; *D. imbricata* is found in Sample 5/2–76, with the stratigraphic interval constrained to the upper Cenomanian–Coniacian; *D.* cf. *algeriana* is characteristic only of the upper Cenomanian–Turonian deposits (Caron, 1985).

The PF complex discussed above allows us to distinguish the layers with *Whiteinella*/*Dicarinella* in the interval of Sample 3/2–72; the ages of these taxa correspond to the late Cenomanian?–Turonian and, probably, the beginning of the Coniacian Stage.

Beginning from Sample 73, rocks constantly contain shells of the *Archaeoglobigerina* genus, which includes three species. These are primitive morphotypes without intense ornamentation, although the *A. cretacea* (d'Orbigny) species has two bands, resembling "undeveloped" keels, on their peripheral rims. The aperture is umbilical, ranging from medium to wide in size, sometimes protected with a plate. Also here, beginning from the level of Sample 73, single representatives of the *Marginotruncana* genus (*M. marginata* Reuss) are found; beginning from the level of Sample 45, *M. pseudolinneiana* Pessagno and *M.* sp. appear, and their morphology is more complex: clearly expressed double keel, a wide aperture covered with plates (porches), and sculptured sutures. The distribution of species from the *Marginotruncana* genus is limited to the Turonian and Santonian deposits, but single shells can be found in deposits of the lower part of the Campanian (Coccioni and Premoli Silva, 2015; Kopaevich and Vishnevskaya, 2016; Vishnevskaya et al., 2018). The ages of the distinguished layers correspond to the Coniacian and Santonian stages.

Apart from spirally conic or trochoid PF shells (globotruncanids), in the KB-1 section, we found shells of spirally screw heterohelicids. They were defined using an applied taxonomy. Heterohelicids are nonuniformly distribution over the section and demonstrate a low diversity (six species): *Heterohelix paraglobulosa* Georgescu et Huber, *H. reussi* (Cushman), *H. papula* (Belford), *H. directa* (Aliyulla), *Pseudoguembelina praehuberi* Georgescu, and *H. striata* (Ehrenberg) (Figs. 5, 7; Plate VI).

The analysis of the distribution of studied taxa has allowed us to find for the first time the stratigraphic sequence of six layers with heterohelicids (Fig. 5, from bottom to top): layers with *Heterohelix paraglobulosa*; layers with *H. reussi*, distinguished from the first appearance of the index species (monospecies layers corresponding to the Cenomanian–Turonian); layers with *H. papula*; layers with *H. directa*; and layers with *Pseudoguembelina praehuberi*, distinguished from the distribution of index species, corresponding to the Turonian. The overlying layers with *H. paraglobulosa*/*H. reussi*/*H. papula* are revealed from the joint distribution of these three species and dated back to the Coniacian. In the upper part of the section, we found singular shells of *H. striata* (Cushman).

Quantitative relationships within foraminiferal complexes, in particular, the PF/BF ratio, indicate the predominance of shallow-water settings in the southern Ulyanovsk-Saratov trough. In terms of this ratio, the section can be clearly subdivided into two intervals. In the Turonian and, partially, lower Coniacian intervals, the PF content is up to 50–60%, whereas it generally ranges between 39 and 60% (Fig. 5). Up the section, the PF content abruptly decreases, not exceeding 10–20%, only in few cases reaching 30%. The relationships between the particular PF morphological groups also vary. In the lower part of the section (Turonian Stage), the content of spirally conic (trochoid) globotruncanid shells ranges from 40 to 100% (Fig. 7, Sample 2/2–73). Up the section, spirally screw heterohelicid shells dominate, with the stable content of 60–70%. This is related to the transgression from the Tethys Ocean that began at the end of the early–the beginning of the middle Turonian, continued in the Coniacian, and led to certain deepening of sedimentary basins and optimization of water temperature (Alekseev et al., 2005; Baraboshkin et al., 2004; Kopaevich and Vishnevskaya, 2016), providing the favorable environment for plankton.

Plate VI. Planktonic foraminifera from the KB-1 section. (1) *Dicarinella algeriana* (Caron), specimen SGU no. 260/BK-2-09, layer 3, middle–upper Turonian; (2) *Whiteinella archaeocretacea* Pessagno, specimen SGU no. 260/BK-2-03, layer 2, middle–upper Turonian; (3) *Whiteinella aumalensis* (Sigal), specimen SGU no. 260/BK-2-03, layer 3, middle–upper Turonian; (4) *Globoheterohelix paraglobulosa* Georgescu et Huber, specimen SGU no. 260/BK-2-06, layer 3, middle–upper Turonian; (5) *Globoheterohelixpara globulosa* Georgescu et Huber, specimen SGU no. 260/BK-2-04, top of layer 2, middle–upper Turonian; (6) *Pseudoplanoglobulina directa* (Aliyulla), specimen SGU no. 260/BK-1-64, layer 4, lower Coniacian; (7) *Heterohelix reussi* (Cushman), specimen SGU no. 260/BK-2-08, layer 3, middle–upper Turonian; (8) *Heterohelix reussi* (Cushman), specimen SGU no. 260/BK-1-01, layer 10, lower Santonian; (9) *Heterohelix reussi* (Cushman), specimen SGU no. 260/BK-2-13, layer 3, middle–upper Turonian; (10) *Heterohelix papula* (Belford), specimen SGU no. 260/BK-1-31, lower part of layer 6, lower Coniacian; (11) *Pseudoplanoglobulina directa* (Aliyulla), specimen SGU no. 260/BK-1-80, layer 3. middle–upper Turonian. (12) *Huberella praehuberi* Georgescu, specimen SGU no. 260/BK-1-71, layer 4, lower Coniacian; (13) *Huberella praehuberi* Georgescu, specimen SGU no. 260/BK-1-45, layer 4, lower Coniacian; (14) *Archaeglobigerina cretacea* d'Orbigny, specimen SGU no. 260/BK-1-76, top of layer 3, middle–upper Turonian; (15) *Whiteinella baltica* Douglas et Rankin, specimen SGU no. 260/BK-1-78, layer 3, middle–upper Turonian; (16) *Whiteinella paradubia* (Sigal), specimen SGU no. 260/BK-1-81, layer 3, middle–upper Turonian; (17) *Archaeglobigerina bosquensis* Pessagno, specimen SGU no. 260/BK-1-74, base of layer 4, lower Coniacian; (18) *Marginotruncana pseudolinneiana* Pessagno, specimen SGU no. 260/BK-1-45, layer 4, lower Coniacian; (19) *Archaeglobigerina blowi* Pessagno, specimen SGU no. 260/BK-1-01, layer 10, lower Santonian; (20) *Marginotruncana marginata* (Reuss), specimen SGU no. 260/BK-1-02, layer 9, lower Santonian. Letter indices at numbers of images denote (a) view from dorsal side, (b) view from ventral side, and (c) view from aperture side. Scale bar is 100 μm.

Plate VI

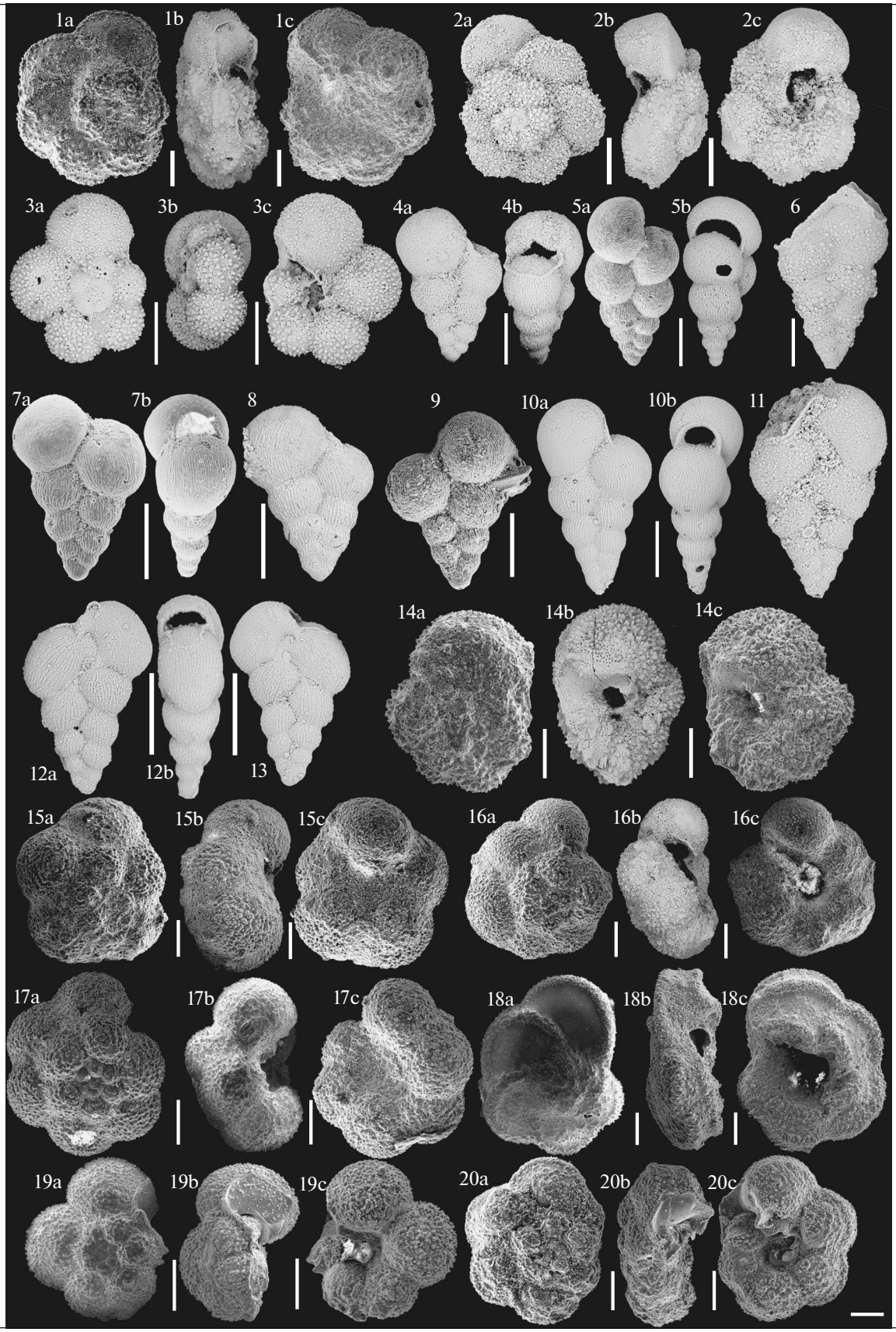
1a
1b
1c
2a
2b
2c
3a
3b
3c
4a
4b
5a
5b
6
7a
7b
8
9
10a
10b
11
12a
12b
13
14a
14b
14c
15a
15b
15c
16a
16b
16c
17a
17b
17c
18a
18b
18c
19a
19b
19c
20a
20b
20c

Radiolarians

The radiolarian complex is extremely scarce (Plate 2) because the studied KB-1 section is represented by carbonate rocks. In layer 9, the EEP zonal species of the lower Santonian, *Quasieuchitonia santonica*, is found (Olfer'ev et al., 2007). Except for the zonal species, this layer also contains *Crucella aster* (Lipman) and *C. membranifera* (Lipman) which, analogous to *Quasieuchitonia santonica* (Lipman), are the representetives of the temperate boreal zone. The radiolarian assemblage includes *Dictyomitra formosa* Squinabol, which is a warm-water species characteristic of the Cenomanian–Turonian of the Mediterranean; however, its geographic range in the Coniacian–Early Santonian spread to the Moscow region of the EEP and Sava River basin in Serbia (Vishnevskaya and Djerič, 2009).

In layer 3, we defined radiolarians *Cavaspongia* sp. and *Crucella* sp. In Samples 78/1 and 5/2 we found *Spongopyle ecleptos* Renz and *Amphipyndax stocki* (Campbell et Clark), respectively. The former is characteristic of the Australian zone and is widespread in Albian–Coniacian deposits of Crimean–Caucasian region and in south of the EEP; the latter is a cosmopolite for the Late Cretaceous. In layer 1, we defined only cancellous discoid *Orbiculiforma* sp. and *Porodiscus* sp. of a broad age interval (Vishnevskaya, 2001).

RESULTS OF PETROMAGNETIC STUDIES

The studied deposits of the KB-1 section appeared to be very weakly magnetic, and in some cases diamagnetic: K ranges from -0.16×10^{-5} to 4.2×10^{-5} SI units; $\mathbf{J_n}$ does not exceed 0.06×10^{-3} A/m (Fig. 8).

The results of magnetic saturation (Fig. 9a) mark the magnetically soft phase typical of finely dispersed magnetite (in all specimens, saturation takes place in the fields of up to 100 mT; $\mathbf{H_{cr}}$ ranges mainly from 30 to 40 mT). The presence of magnetite is unambiguously indicated by thermomagnetic analysis (TMA): the magnetic susceptibility clearly drops in the vicinity of the Curie temperature of this mineral—578°C (Fig. 9b).

The stereographic distribution of AMS ellipsoid axes appears to be generally chaotic throughout the section (Fig. 9c); most likely, this reflects random measurement errors, because the possible effect of anisotropy in weakly magnetic specimens is below the threshold sensitivity of the instrument. In the most "intensely magnetic" ($K > 1 \times 10^{-5}$ SI units) specimens, we revealed the tendency of projections of the short axes (*K3*) to the group in southern sectors of stereogram (Fig. 9d). This regularity probably reflects the primary magnetic structure of sediments, and preservation of this structure is favorable for paleomagnetic studies. In the absence of disturbances in the sedimentation medium, the minor axes of flat particles are arranged vertically, whereas the long (*K1*) and middle (*K2*) axes are arranged horizontally (Tarling and Hrouda, 1993). Weak ordering of *K3* and their significant deviation from the mean direction from the center of polar stereogram can be caused by arbitrary shape of magnetic particles, as documented on the P–T diagram (Tarling and Hrouda, 1993) (Fig. 9d).

Low values of the Q factor (<0.5) observed throughout the entire section (Fig. 8) are typical of the detrital (post-detrital) magnetization. This is also a favorable condition for paleomagnetic studies, because orientational genesis of magnetization is a synonym of its primary character. The only level (Sample KB-1/36) possessing a high value of Q (2.1), which is not characteristic of the orientational nature of $\mathbf{J_n}$, coincides with the surface of a sedimentation hiatus, on which we should expect the presence of authigenic ferromagnetic substances carrying chemical magnetization.

The section is differentiated in a petromagnetic sense (Fig. 8). The bottom of layer 7 and top of layer 8 are characterized by noticeable increases in $\mathbf{J_n}$ and Q indicating a higher degree of ordering of ferromagnetic particles in this interval. In the case of orientational (post-orientational) nature of magnetization, the similar effect is often related to the decrease in size of the ferromagnetic fraction, because fine particles are more easily oriented along the geomagnetic field. However, parameter $K/\mathbf{J_{rs}}$ representing the average size of ferromagnetic grains does not demonstrate, excluding isolated cases, significant variations along the sections, suggesting that ferromagnetic grains were of close sizes. In this case, better orientation of ferromagnetic grains was provided by other factors, such as quiet hydrodynamic settings in near-bottom layers of the paleobasin and/or increase in geomagnetic field intensity.

The uppermost part of the section, beginning from the middle part of layer 5 (Samples KB-1/28 to KB-1/1), is clearly distinct in higher values of K, $\mathbf{J_n}$, $\mathbf{J_{rs}}$, and $\mathbf{H_{cr}}$. The increases in magnetic susceptibility and remanent magnetizations indicate the higher concentrations of ferromagnetic substances. The increase in remanent coercive force, at unchanged size of the ferromagnetic fraction, should be attributed to oxidation of magnetite grains due to oxygen enrichment of the sedimentation medium. The absence of a positive thermokappametric effect ($dK \leq 0$ through the entire section, excluding the bottom of layer 8) indicates that the studied deposits do not contain finely dispersed pyrite and, therefore, formed under an oxidizing environment. The decrease in magnetic susceptibility of specimens upon heating occurs owing to intense oxidation of magnetite grains in them.

RESULTS OF PALEOMAGNETIC STUDIES

The results of magnetic cleanings after $\mathbf{J_n}$ measurements on spinner and SQUID magnetometers demonstrate a good match, at better quality of Zijderveld plots obtained on a SQUID magnetometer (Fig. 10a). Despite small values of $\mathbf{J_n}$, characteristic

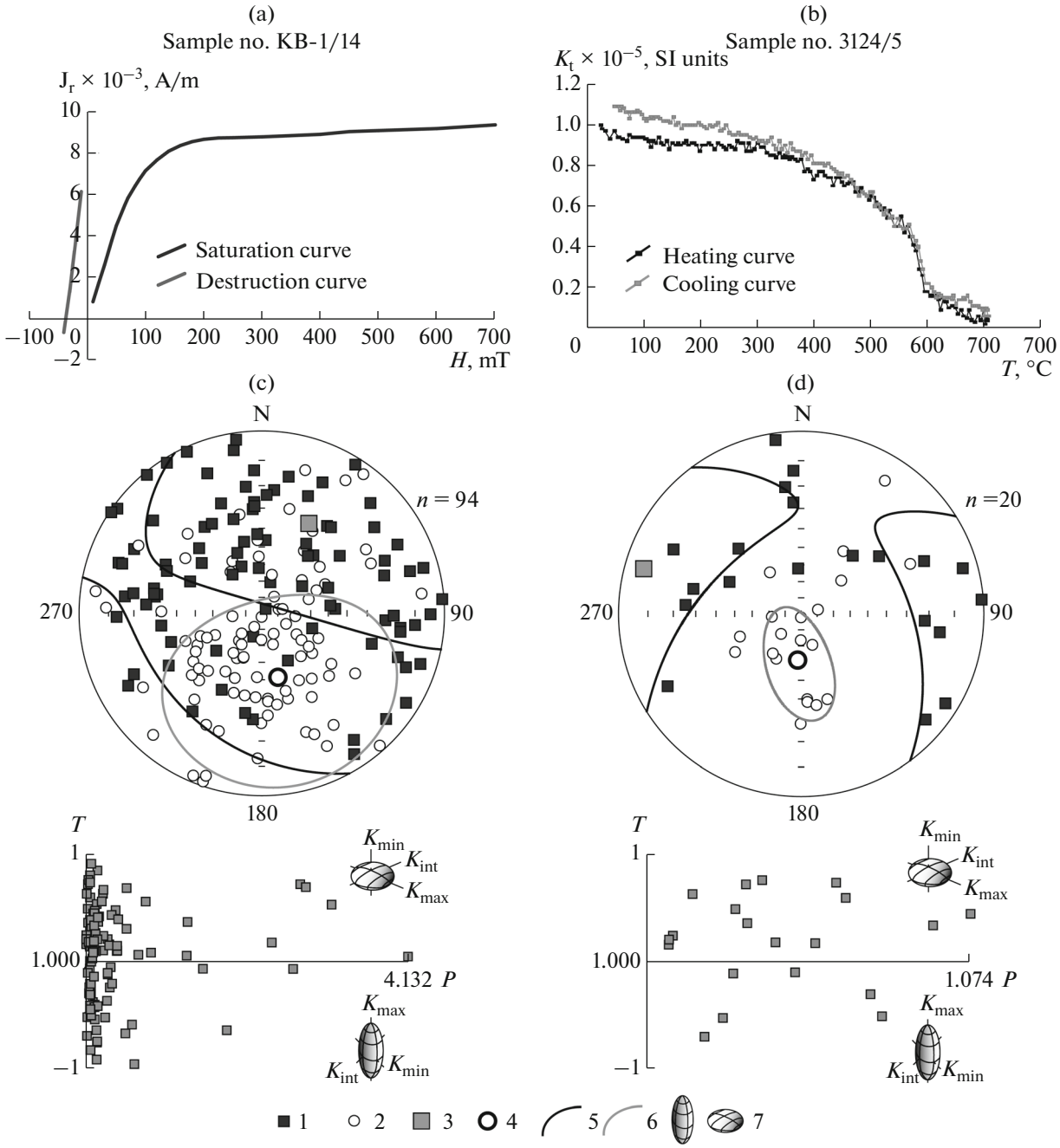

Fig. 9. Results of magneto-mineralogical analysis. (a) Curves of magnetic saturation and destruction; (b) curves of thermomagnetic analysis (TMA); (c, d) AMS data: stereograms of projections of long (*K1*) and short (*K3*) AMS axes in terms of the geographic coordinate system and *P*–*T* diagrams (*P* and *T* denote anisotropy and shape parameters; positive or negative values of *T* indicate predominance of ferromagnetic particles of flattened or elongated shape, respectively) on all samples (c) and on those with $K \geq 1 \times 10^{-5}$ SI units (d). Legend: (1) *K1*; (2) *K3*; (3, 4) mean directions of *K1* and *K3*, respectively; (5, 6) confidence ellipses for mean direction of *K1* and *K3*, respectively; (7) schematic representations of shapes of AMS ellipsoids.

components (**ChRM**) of acceptable quality with the maximum angle of deviation less than 15° (Fig. 10a) have been distinguished in the majority of specimens owing to measurements on a cryogenic magnetometer.

ChRM values, regularly grouping in northern directions of the lower hemisphere of stereographic projection, correspond to the normal (N) polarity of the geomagnetic field (Figs. 10b, 11) and form two large magnetic zones in the section: N1 (bottom of layer 7), supported by samples from nine levels, and N2 (upper half of layer 5 and layer 4), supported by samples from 24 levels (Fig. 11). A single interval of normal polarity is found in the uppermost part of layer 8 (Fig. 11). The N components of magnetization are

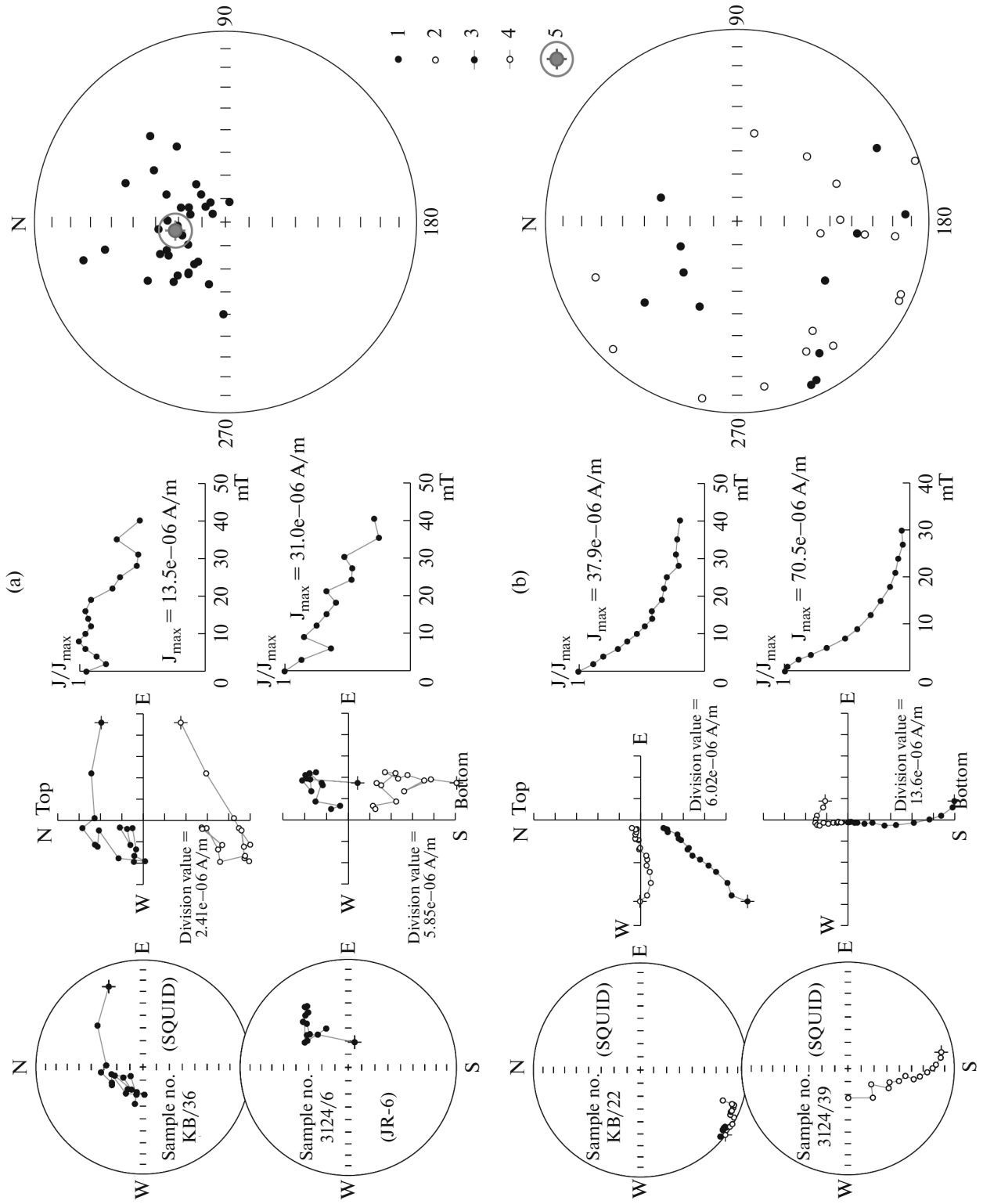

Fig. 10. Results of component analysis of samples. (a) From left to right: stereographic images of variation in $\mathbf{J_n}$ vectors during magnetic cleanings, Zijderveld plots in terms of the geographic coordinate system, and graphs of samples demagnetization; (b) stereographic projections of paleomagnetic directions corresponding to normal polarity; (c) stereographic projections of anomalous directions. "JR-6" and "SQUID" in stereograms mean that the measurements were made on a JR-6 spinner magnetometer (Laboratory of Petrophysics, Saratov State University) and a 2G-Enterprises cryogenic magnetometer (Schmidt Institute of Physics of the Earth, Russian Academy of Sciences), respectively. Legend: (1, 2) projections of $\mathbf{J_n}$ (on stereograms) onto the lower and upper hemispheres, respectively; (3, 4) projections of $\mathbf{J_n}$ (on Zijderveld plots) onto the (3) horizontal and (4) vertical planes; (5) average paleomagnetic direction with a confidence ellipse.

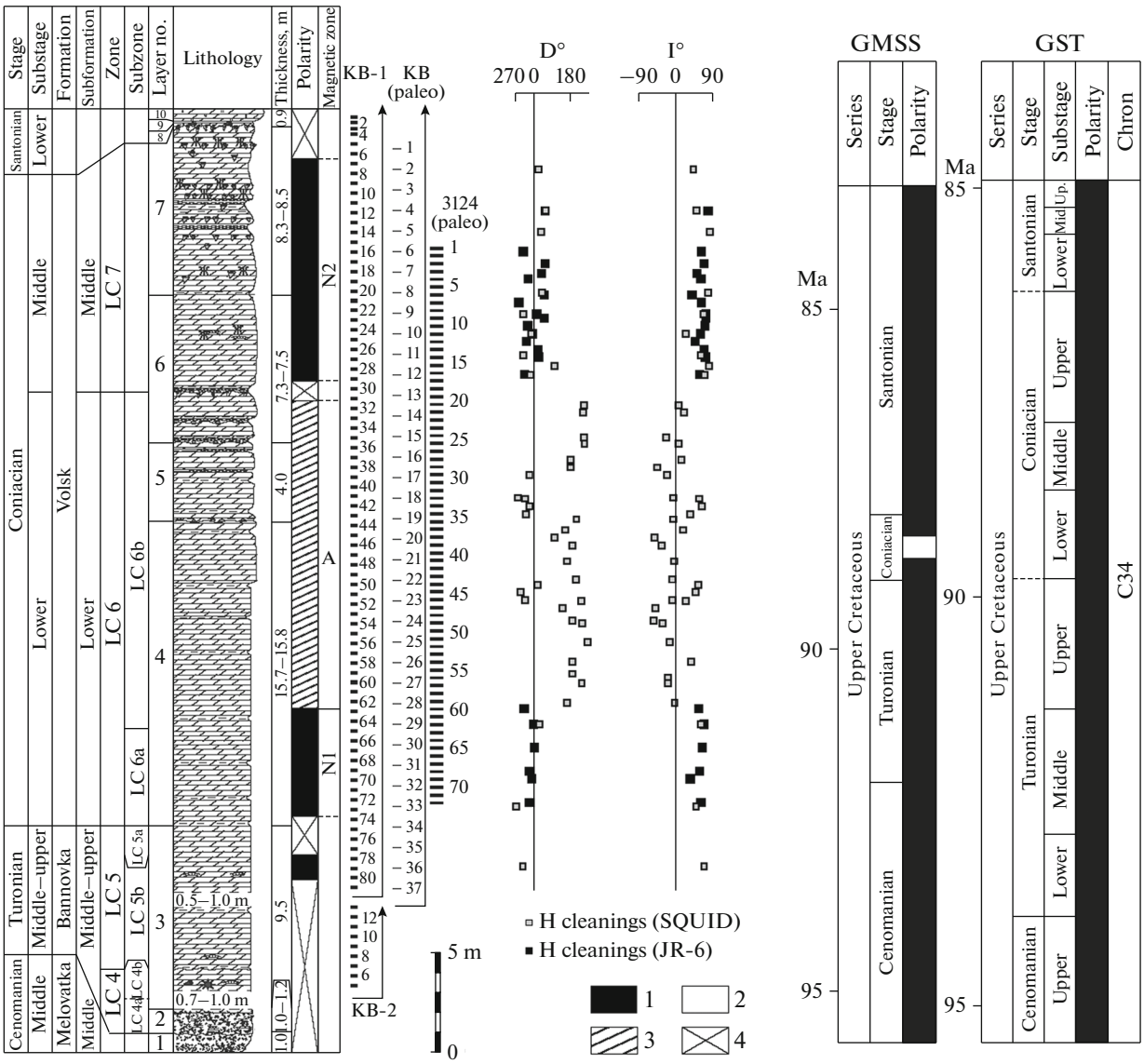

Fig. 11. Paleomagnetic characteristics of the KB-1 section and its comparison with the General Magnetostratigraphic Scale (*Dopolneniya...*, 2000) and Geologic Time Scale (Ogg et al., 2016). Legend: (1–3) geomagnetic polarity: (1) normal, (2) reverse, (3) anomalous; (4) absence of data on polarity. Legend to the lithologic column is the same as Fig. 3.

characterized by good (given the extremely low $\mathbf{J_n}$ values) parameters of paleomagnetic statistics (Table 1). The mean direction of characteristic components ($\mathbf{ChRM_{av}}$) statistically coincides with the vector of the present-day geomagnetic field in the region under study, but this point does not contradict the hypothesis about primary character of magnetization because the directions of Late Cretaceous and present-day fields are close for the Lower Volga region (Table 1). $\mathbf{ChRM_{av}}$ are statistically indistinguishable from the mean paleomagnetic vectors determined earlier on Turonian–Coniacian and Campanian–Maastrichtian deposits of the Volga River right bank in Saratov oblast (Guzhikov et al., 2017; Guzhikova and Beniamovsky, 2018; Guzhikova et al., 2019) and from the direction calculated for the area under study from the paleomagnetic pole coordinates for stable Europe at 85 Ma (Besse and Courtillot, 2002) (Table 1). The inversion test carried out for N directions from the Kamennyi Brod section and R directions from the summarized Ozerki–Lipovka section of Turonian–Coniacian (Santonian?), Saratov part of the Volga region (Guzhikova et al., 2019), appears to be positive: the angle between normalized vectors is 0.2° and the critical angle is 11.2°, corresponding to "C" class after (McFadden and McElchinny, 1990).

The absence of significant differences of $\mathbf{ChRM_{av}}$ for both the mean paleomagnetic vectors of the Late Cretaceous deposits of the Volga River right bank in Saratov oblast and the direction of the field in the

Table 1. Statistical parameters of distributions of paleomagnetic directions (in terms of the stratigraphic coordinate system)

Section/age/polarity				n	D°_{av}	I°_{av}	k	α°_{95}	Angle (°) with **ChRM$_{av}$** (KB)**
Paleomagnetic directions on Upper Cretaceous of Volga River right bank in Volgograd and Saratov oblasts	Kamennyi Brod (present work)	K_2t-k	N	31	352.8	67.1	14.6	7.0	
	Ozerki–Lipovka (Guzhikova et al., 2019)	K_2t-k(st?)	R*	74	350.4	68.1	6.6	7.0	1.4 ± 7.3
	Volsk (Guzhikova and Beniamovsky, 2018)	K_2km	N + R*	72	3.5	63.6	13.1	4.8	4.6 ± 6.4
	Nizhnyaya Bannovka (Guzhikov et al., 2017; Guzhikova et al., 2019)	K_2m	N	59	349.9	65.1	20.9	4.2	2.3 ± 6.2
		K_2km	N	91	3.3	63.1	11.0	4.7	5.0 ± 6.4
		K_2t-k	N	65	349.3	69.0	11.2	5.5	2.3 ± 6.7
Direction of the present-day geomagnetic field in the studied region					0.0	67.0		10.0	2.8 ± 9.0
Field directions in the studied region recalculated from coordinates of the standard Late Cretaceous paleopoles of different ages for stable Europe (Besse and Courtillot, 2002):		75 Ma		10	6.9	61.3		5.3	7.7 ± 6.6
		80 Ma		9	358.3	59.9		7.8	6.8 ± 6.5
		85 Ma		5	358.8	60.0		10.0	6.6 ± 7.3
		90 Ma		8	7.7	61.1		2.6	8.3 ± 5.6
		95 Ma		8	7.4	62.0		4.7	7.4 ± 6.3

R* means R directions normalized to N polarity; **ChRM$_{av}$**(KB)**, direction of characteristic components corresponding to N polarity on the basis of the Kamennyi Brod section; n, number of samples (for paleopoles, number of sites); D_{av} and I_{av} are average paleomagnetic dip and inclination, respectively; k, interlayer paleomagnetic clustering; α_{95}, radius of confidence circle of vector. For the direction of present-day geomagnetic field, n equals the number of outcrops; α_{95} is assumed equal to the maximum amplitude of secular variation (Bakhmutov, 2006). Angles formed by vectors are given with errors (±) determined by statistics of these vectors according to (Debiche and Watson, 1995). If the angle is larger than the error, the vectors differ significantly; otherwise, they statistically coincide.

studied region, recalculated from the standard pole for stable Europe at 85 Ma, along with the positive result of the inversion test, agrees with the hypothesis about the primary character of magnetization components, on whose basis the N1 and N2 magnetic zones were distinguished.

Most magnetization components identified in the middle part of the section tend to the southeastern sector of the sphere and have negative or gentle positive dips. Some of these directions are typical of the reverse polrity mode (R), but many cannot be related to either direct or reverse polarity (Fig. 10c). **ChRM** values measured in specimens collected from 29 levels are close to the directions typical of normal polarity only in five cases (Figs. 10c, 11). The interval of the section where predominantly anomalous $\mathbf{J_n}$ components were recorded (upper half of layer 7, layer 6, and base of layer 5) was distinguished as the magnetic zone of anomalous polarity (A), supported by specimens collected from 29 levels (Fig. 11).

The suggestions about secondary nature of the anomalous magnetic zone imply the possibility of selective remagnetization in the section. Insignificant differentiation of the material composition and physical properties of the studied rocks poorly agrees with such a suggestion. If the observed differences are really the reason for remagnetization, then the A magnetic zone should be unique in lithologic and petromagnetic aspects, but this is not true. In theory, it is possible that the interval of the section with anomalous magnetization marks the record of some ancient (Late Cretaceous) field characteristic of epochs of geomagnetic excursions. However, the duration of excursions does not exceed several hundred years to a thousand years (*Encyclopedia*..., 2007), and it seems very unlikely that the carbonate sequence 20 m thick formed in such a short period.

Finally, anomalous components of magnetization can represent a stabilized vector sum of normal and reverse polarity components. In this case, we can suppose that the normal component is related to partial remagnetization by the present-day field, and the reverse component is the ancient (primary) one. Given the lithologic and petromagnetic differentiation of the section, we should assume possible partial remagnetization, to a greater or lesser degree, for all studied deposits. However, as the directions of Late Cretaceous and present-day fields are close, it is impossible to differentiate the respective components

in specimens hosting the primary magnetization component caused by normal polarity.

Thus, the most probable interpretation of the obtained paleomagnetic data is that the interval of deposits corresponding to the anomalous magnetic zone formed in the reverse polarity epoch. The presence of anomalous directions is explained by the impossibility to separate the ancient R component and stabilized viscous component caused by the present-day field during magnetic cleaning.

CONCLUSIONS

(1) The Turonian–Coniacian boundary in the KB-1 section has been revealed only from the studies of BF complexes; the intraformation hiatus here is barely expressed in a thin interbed of argillic marl. The intervals of the upper part of the Turonian corresponding to the LC5b and LC5c BF-based subzones have not been revealed in the section. The base of lower Coniacian (base of LC6 Zone) has been determined from the first appearances of *Pseudovalvulineria kelleri kelleri* (Mjatluk) and *Stensioeina emscherica* Baryschnikova. This zone is traced over large area of the European paleobiogeographic region (Beniamovsky, 2008a). The thickness of carbonate rocks of the Volsk Formation (Coniacian) in the KB-1 section is estimated at 35–36 m, of which 22 m corresponds to the lower subformation and 13 m to the middle one; the thickness of the Bannovka Formation (Turonian) is 10–12 m, of which the carbonate part is about 9–10 m thick.

(2) The KB-1 section can be recommended for consideration as a hypostratotype of the Volsk Formation because it is the most stratigraphicaly full and sequential. The holostratotype of the Volsk Formation, at the Krasnyi Oktyabr' quarry (Volsk), contains only rocks from the upper subformation up to 2.5–3 m thick, with ambiguously interpreted boundaries with underlying and overlying units. In the Nizhnyaya Bannovka section, the Volsk Formation is represented by marls of the lower subformation up to 4–5 m thick. Many sections of Volga River right bank, where carbonate rocks of the Gubkino Horizon are reported, the Volsk Formation has not been reliably distinguished.

(3) Coniacian rocks are characterized by a more widespread lateral distribution than was believed earlier. Analysis of the thickness of carbonate rocks at the level of subformations, coupled with analysis of the ratio between BF and PF, gives grounds to suggest that the maximum manifestation of transgression in the southern Ulyanovsk-Saratov trough in Gubkino time fell within the Early Volsk phase.

(4) Reconstruction of the regional structural plan in pre-Santonian time caused the absence of Coniacian rocks in the greater part of the present-day Volga region. The "sponge" horizons revealed in Middle Coniacian marls of the KB-1 section indicate the initial phase of succession of siliceous sponges in the region. The composition and structure of the Santonian "sponge" horizon reflect the events of the mature and late stages of succession; occasionally, it also contains redeposited fossils from Cenomaian–Coniacian rocks.

(5) The level of concentrated burials of echinoderms has been identified in Turonian marls of the KB-1 section; this level is traced in sections of the southwestern Ulyanovsk-Saratov trough (Chukhonastovka-1, Chukhonastovka-2, and Splavnukha-1). The ideas about species diversity of four classes of Late Cretaceous Echinodermata and regularities of their distribution in the region have been expanded (Kalyakin, 2015, 2017). Among Turonian communities reported within the territory of the European part of Russia, this echinoderm complex is distinct in the highest representativeness. The earliest (Turonian) appearance of *Nielsenicrinus carinatus* (Roemer) crinoids has been revealed.

(6) Magnetopolar data on the KB-1 section contradict those on the exclusively normal polarity mode of the geomagnetic field in Cenomanian–Santonian time, reflected in the Geologic Time Scale (Ogg et al., 2016) (Fig. 11); however, they support an alternative point of view about the existence of a reverse polarity epoch in the Coniacian Stage, reflected in the General Magnetostratigraphic Scale (GMSS) (*Dopolneniya*..., 2000). If our hypotheses about the primary character of magnetization and the stipulation that anomalous directions were caused reverse polarity mode are true, then the A magnetic zone should be matched with the Klyuevskaya R zone located in the middle of the Coniacian Stage on the GMSS (*Dopolneniya*..., 2000) (Fig. 11). Note that the stratigraphic position of the Klyuevskaya R zone is specified for the first time: in the studied section, it occurs in the uppermost part of the lower Coniacian substage.

It was found earlier that the deposits which the Stratigraphic Scheme of the Upper Cretaceous of the EEP (2004) refers to the Turonian–Santonian in the area of the villages of Ozerki and Lipovka (Lysogorsk district of Saratov oblast) were characterized by reverse polarity (Guzhikova et al., 2019; Pervushov et al., 2017a, 2017b). This agrees in part with the data from the KB-1 section about the presence of a reverse polarity magnetic zone in the Coniacian Stage, but the R zone in Ozerki covers deposits ascribed by microfaunal finding to the middle–upper Coniacian.

It seems unreasonable to revise the age of deposits or draw a conclusion about significant diachronicity of boundaries validated by microfauna, at least on the basis of the available data, before new comprehensive (bio- and magnetostratigraphic) data are obtained on other Upper Cretaceous sections of Volga region and adjacent areas. On the contrary, the necessity of these studies is clear, because if the point of view about the presence of a long-term reverse polarity epoch in the Turonian–Coniacian were supported, it would have significant geophysical and stratigraphic implications.

Specification of the Late Cretaceous field mode is topical from the perspective of geomagnetic dynamo theory. In terms of stratigraphy, new R zones are valuable references of isochronous nature for interregional and global correlations.

ACKNOWLEDGMENTS

We thank A.G. Manikin and V.A. Grishchenko (Saratov State University) for participation in the field study of the section; V.E. Pavlov, R.V. Veselovskii, and other members of the Laboratory for Principal Geomagnetic Field and Petromagnetism (Schmidt Institute of Physics of The Earth, Russian Academy of Sciences) for the opportunity to conduct measurements on a cryogenic magnetometer; A.M. Zakharevich (Laboratory for Materials Nanodiagnostics, Educational and Scientific Institute of Nanostructures and Biosystems, Saratov State University); and D.M. Georgesku. We are also grateful to A.S. Alekseev and A.P. Ippolitov for determination of invertebrates from the Chukhonastovka-2 section.

FUNDING

This work was supported by the Russian Foundation for Basic Research (project nos. 18-05-00784-a and 18-05-00503) and carried out within the framework of scheduled research of the Geological Institute, Russian Academy of Sciences (project no. 0135-2018-0036).

Reviewers E.Yu. Baraboshkin and V.A. Zakharov

REFERENCES

Akimets, V.S., Detailed foramiferal biostratigraphy of the Cretaceous deposits in the Polesia saddle, in *Novoe o geologicheskom stroenii territorii BSSR. Sb. nauchn. tr.* (New Data on the Geological Structure of the BSSR. Coll. Sci. Works), Minsk: BNIGGI, 1981, pp. 83–101.

Alekseev, A.S., Kopaevich, L.F., Baraboshkin, E.Yu., Gabdullin, R.R., Olfer'ev, A.G., and Yakovishina, E.V., Paleogeography of the southern part of the East European Platform and its folded frame in the Late Cretaceous. Part 2: Paleogeographic setting, *Byull. Mosk. O-va Ispyt. Prir., Otd. Geol.*, 2005, vol. 80, no.4, pp. 30–44.

Aliev, M.M. and Kharitonov, V.M., Upper Cretaceous inocerams, in *Melovaya fauna Azerbaidzhana* (Cretaceous Flora of Azerbaijan), Baku: El'm, 1988, pp. 250–273.

Arkhangelsky, A.D., About Cretaceous and Tertiary deposits of the Kamyshin Uyezd, Saratov Province. Study report for 1905, in *Materialy dlya geologii i mineralogii Rossii* (Materials on the Geology and Mineralogy of Russia), 1908, vol. 23, no. 2, pp. 431–489.

Arkhangelsky, A.D., Upper Cretaceous deposits of the eastern part of the European Russia, in *Materialy dlya geologii Rossii* (Materials on the Geology of Russia), 1912, vol. 25, no. 2, pp. 431–489.

Arkhangelsky, A.D. and Dobrov, S.A., Geological essay of the Saratov Province, in *Materialy izucheniya estestvenno-proizvoditel'nykh uslovii Saratovskoi gubernii. Vyp. 1* (The Data on Studying the Natural–Historical Conditions in the Saratov Province. Vol. 1), Moscow: Pechatnya S. Yakovleva, 1913 [in Russian].

Bakhmutov, V.G., *Paleovekovye geomagnitnye variatsii* (Paleosecular Geomagnetic Variations), Kiev: Naukova Dumka, 2006 [in Russian].

Baraboshkin, E.Yu., Alekseev, A.S., and Kopaevich, L.F., Cretaceous palaeogeography of the North-Eastern PeriTethys, *Palaeogeogr., Palaeoclimatol., Palaeoecol.*, 2004, vol. 196, no. 2, pp. 177–208.

Baryshnikova, V.I., Foraminiferal stratigraphy of Upper Cretaceous deposits in the Middle Don River, in *Tez. dokl. Nauchn. konf. po stratigrafii mezozoya i paleogena Nizhnego Povolzh'ya* (Proc. Sci. Conf. on Mesozoic and Paleogene Stratigraphy of the Low Volga Region), Saratov: Saratov. Gos. Univ., 1955, pp. 62–64.

Baryshnikova, V.I., The foraminiferal stratigraphic subdivision of the Upper Cretaceous deposits in the Middle Don River, in *Tr. Vsesoyuz. soveshch. po razrabotke unifitsirovannoi skhemy stratigrafii mezozoiskikh otlozhenii Russkoi platformy* (Proc. All-Union Conf. on Development of Unified Stratigraphic Scale for the Mesozoic Deposits of the Russian Platform), Leningrad: GNTI–NGTL, 1956, pp. 269–275.

Baryshnikova, V.I., On the subdivision of the Turonian–Coniacian deposits in the Middle Don River, in *Uch. zap. SGU im. N.G. Chernyshevskogo* (Trans. Chernyshevsky Saratov State Univ.), Saratov: Saratov. Gos. Univ., 1959, vol. 65, pp. 65–77.

Baryshnikova, V.I., Ivanova, A.N., Morozov, N.S., and Khabarova, T.N., Stratigraphy of the Upper Cretaceous deposits of the Saratov and Stalingrad Volga Regions, in *Mater. Vsesoyuzn. soveshch. po utochneniyu unifitsirovannoi skhemy stratigrafii mezozoiskikh otlozhenii Russkoi platformy. Tr. VNIGNI. Vyp. 29* (Proc. All-Union Conf. on Development of Unified Stratigraphic Scale for the Mesozoic Deposits of the Russian Platform. Trans. All-Russ. Petrol. Res. Inst. Vol. 29), 1961, vol. 3. pp. 110–119.

Beniamovsky, V.N., Infrazonal biostratigraphy of the Upper Cretaceous in the East European province based on benthic foraminifers, Part 1: Cenomanian–Coniacian, *Stratigr. Geol. Correl.*, 2008a, vol. 16, no. 3, pp. 257–266.

Beniamovsky, V.N., Infrazonal biostratigraphy of the Upper Cretaceous in the East European province based on benthic foraminifers, Part 2: Santonian–Maastrichtian, *Stratigr. Geol. Correl.*, 2008b, vol. 16., no. 5, pp. 515–527.

Besse, J. and Courtillot, V., Apparent and true polar wander and the geometry of the geomagnetic field over the last 200 Myr, *J. Geophys. Res.*, 2002, vol. 107, no. 11, pp. 1–31.

Bondareva, M.V. and Morozov, N.S., Cenomanian, Turonian, and Coniacian deposits of the Medveditsa–Volga watershed within the Volga right bank region, in *Voprosy geologii Yuzhnogo Urala i Povolzh'ya. Vyp. 24* (Problems of Geology of the Southern Urals and Volga Region. Vol. 24), Saratov: Saratov. Gos. Univ., 1984, pp. 62–70.

Caron, M., Cretaceous planktonic foraminifera, in *Plankton Stratigraphy*, Bolli, H.M., Saunders, J.B., and Perch-Nielsen, K., Eds., Cambridge: Cambridge Univ. Press, 1985, pp. 17–86.

Coccioni, R. and Premoli Silva, I., Revised Upper Albian-Maastrichtian planktonic foraminiferal biostratigraphy and magnetostratigraphy of the Classical Tethyan Gubbio section, *Newsl. Stratigr.*, 2015, vol. 48, no. 1, pp. 47–90.

Debiche, M.G. and Watson, G.S., Confidence limits and bias correction for estimating angles between directions with applications to paleomagnetism, *J. Geophys. Res.*, 1995, vol. 100, no. B12, pp. 24405–24430.

Dobrov, S.A. and Pavlova, M.M., Inocerams, in *Atlas verkhnemelovoi fauny Severnogo Kavkaza i Kryma* (Atlas of Upper Cretaceous Fauna from the North Caucasus and Crimea), Moscow: Gostoptekhizdat, 1959, pp. 130–165.

Dopolneniya k Stratigraficheskomu kodeksu Rossii (Supplements to the Stratigraphic Code of Russia), St. Petersburg: Vseross. Nauchno-Issled. Geol. Inst., 2000 [in Russian].

Dubicka, Z. and Peryt, D., Classification and evolutionary interpretation of late Turonian–early Campanian Gavelinella and Stensioeina (Gavelinellidae, benthic foraminifera) from western Ukraine, *J. Foraminiferal Res.*, 2014, vol. 44, pp. 151–176.

Encyclopedia of Geomagnetism and Paleomagnetism, Springer, 2007.

Gosudarstvennaya geologicheskaya karta Rossiiskoi Federatsii. Masshtab 1 : 1000000 (tret'e pokolenie). Seriya Tsentral'no-Evropeiskaya. List M-38 – Volgograd. Ob"yasnitel'naya zapiska (The 1 : 1000000 State Geological Map of the Russian Federation, 3rd ed. Ser. Central European. Sheet M-38–Volgograd. Explanatory Note), St. Petersburg: Kart. Fabr. Vseross. Nauchno-Issled. Geol. Inst., 2009 [in Russian].

Guzhikov, A.Yu., Geological informativeness of magnetic properties of the core and sludge of sedimentary rocks from exploration well logs, *Devices and Systems of Exploration Geophysics,* 2013, no. 4 (46), pp. 51–61.

Guzhikov, A.Yu., Baraboshkin, E.Yu., Beniamovsky, V.N., Vishnevskaya, V.S., Kopaevich, L.F., Pervushov, E.M., and Guzhikova, A.A., New bio- and magnetostratigraphic data on Campanian–Maastrichtian deposits of the classical Nizhnyaya Bannovka section (Volga River right bank, Southern Saratov Region), *Stratigr. Geol. Correl.*, 2017a, vol. 25, no. 1, pp. 39–75.

Guzhikov, A.Yu., Guzhikova, A.A., Pervushov, E.M., Ryabov, I.P., Sel'tser, V.B., Surinskiy, A.M., and Beniamovsky, V.N., The reverse polarity zone in Turonian–Coniacian of the Lower Volga region (Saratov and Volgograd regions, Russia), in Abstr. *10th Int. Symp. on the Cretaceous, August, 21–26, 2017, Vienna*, Sames, B., Ed., Vienna: Berichte der Geologischen Bundesanstalt, 2017b.

Guzhikova, A.A. and Beniamovsky, V.N., The Campanian–Maastrichtian magnetostratigraphy of the Volga Region (vicinity of Volsk town), *Russ. Geol. Geophys.*, 2018, vol. 59, no. 3, pp. 276–284.

Guzhikova, A.A., Guzhikov, A.Y., Pervushov, E.M., Ryabov, I.P., and Surinskiy, A.M., Existence of the reversal polarity zones in Turonian–Coniacian from the Lower Volga (Russia): new data, in *Recent Advances in Rock Magnetism, Environmental Magnetism and Paleomagnetism*, Nurgaliev, D., Shcherbakov, V., Kosterov, A., Spassov, S., Eds., Springer Geophys. Springer, Cham, 2019, pp. 353–369.

Kalyakin, E.A., The history of studying echinoids from the Upper Cretaceous deposits of the Volga Region, *Izv. Saratov. Gos. Univ. Nov. Ser. Ser. Nauki o Zemle*, 2015, vol. 15, vol. 1, pp. 37–45.

Kalyakin, E.A., Late Cretaceous echinoids of the Central Russian Paleobiogeographic Realm, in *Problemy paleoekologii i istoricheskoi geoekologii. Sb. trudov Vseross. nauchn. konf., posvyashchennoi pamyati prof. V.G. Ocheva* (Proc. All-Russ. Sci. Conf. Devoted to the Memory of V.G. Ochev "Problems of Paleoecology and Historical Geoecology"), Saratov: Saratov. Gos. Tekh. Univ., 2017, pp. 90–96.

Kamysheva-Elpatievskaya, V.G. and Kuznetsova A.M., On the paleontologically characterized Coniacian deposits in the Donskaya Luka locality, *Uch. Zap. Saratov. Gos. Univ. Vyp. Geol.*, 1951, vol. 28, pp. 209–211.

Kats, Yu.I., The phylum Brachiopoda – Brachiopods, in *Atlas verkhnemelovoi fauny Donbassa* (Atlas of Upper Cretaceous of Donbas), Moscow: Nedra, 1974, pp. 240–275.

Kaufman, E.G., Kennedy, W.J., and Wood, C.J., Coniacian stage and substage boundaries, in *Proc. Int. Symp. on Cretaceous Stage Boundaries, Brussels, September, 8–16, 1995, Bull. l'Inst. Royal Sci. Natur. Belgique*, 1996, vol. 66, pp. 81–94.

Klikushin, V.G., Crinoids from the Upper Cretaceous deposits of the USSR, *Byull. Mosk. O-va Ispyt. Prir., Otd. Geol.*, 1980, vol. 55, no. 5, pp. 80–84.

Klikushin, V.G., On the Late Cretaceous crinoids from the Mangyshlak, *Paleontol. Zh.*, 1982, vol. 4, pp. 98–103.

Klikushin, V.G., *Iskopaemye morskie lilii pentakrinidy i ikh rasprostranenie v SSSR* (Fossil Pentacrinid Crinoids and Their Distribution in the USSR), St. Petersburg: Leningrad. Paleontol. Lab., 1991 [in Russian].

Koch, W., Stratigraphie der Oberkreide in Nordwestdeutchland (Pompeckjsche Scholle). Teil 2. Biostratigraphie in der Oberkreide und taxonomie von foraminiferen, *Geol. Jahrb.*, 1977, vol. 38, pp. 11–123.

Kopaevich, L.F. and Vishnevskaya, V.S., Cenomanian–Campanian (Late Cretaceous) planktonic assemblages of the Crimea-Caucasus area: palaeoceanography, palaeoclimate and sea level changes, *Palaeogogr., Palaeoclimatol., Palaeoecol.*, 2016, vol. 441, Spec. Iss., pp. 493–515.

Košták, M., Cenomanian trough the lowermost Coniacian Belemnitellidae Pavlow (Belemnitida, Coleoidea) of the East European Province, *Geolines*, 2004, vol. 18, pp. 59–103.

Lach, R. and Salamon, M.A., Late Cretaceous crinoids (Echinodermata) from the southwestern margin of the Holy Cross Mts. (southern Poland) and phylogenetic relationships among bourgueticrinids, *Paläontol. Z.*, 2016, vol. 90, no. 3, pp. 503–520.

Loeblich, A.R. and Tappan, H.N., *Foraminiferal Genera and Their Classification*, New York: Van Nostrand Reinhold Comp., 1988.

Makhlin, V.Z., Subclass Endocochlia, in *Novye vidy drevnikh rastenii i bespozvonochnykh SSSR. Tr. VNIGRI. Vyp. 318* (New Species of Ancient Plants and Invertebrates of the USSR. Trans. All-Russ. Petrol. Res. Inst. Vol. 318), 1973, pp. 87–92.

Mazarovich, A.N., On the Upper Cretaceous deposits in the Ilovlya River basin (Saratov Province), *Byull. Mosk. O-va Ispyt. Prir., Otd. Geol.*, 1924, vol. 2, no. 3, pp. 1–10.

McFadden, P.L. and McElchinny, M.W., Classification of the reversal test in palaeomagnetism, *Geophys. J. Int.*, 1990, vol. 103, pp. 725–729.

Milanovskii, E.V., *Ocherk geologii Srednego i Nizhnego Povolzh'ya* (Essay on Geology of Middle and Low Volga Regions), Moscow–Leningrad: Gostoptekhizdat, 1940 [in Russian].

Molostovskii, E.A. and Khramov, A.N., *Magnitostratigrafiya i ee znachenie v geologii* (Magnetostratigraphy and its Sig-

nificance for Geology), Saratov: Saratov. Gos. Univ., 1997 [in Russian].

Morozov, N.S., Geological structure of the Medveditsa–Ilovlya interfluve in the northern part of the Stalingrad Oblast, *Uch. Zap. Saratov. Gos. Univ., Vyp. Geol.*, 1951, vol. 28, pp. 117–136.

Morozov, N.S., New data of the stratigraphy of Upper Cretaceous deposits from the Ilovlya, Medveditsa, Khopr and Don right bank regions, in *Tr. Vsesoyuz. soveshch. po razrabotke unifitsirovannoi skhemy stratigrafii mezozoiskikh otlozhenii Russkoi platformy* (Proc. All-Union Conf. on Development of Unified Stratigraphic Scale for the Mesozoic Deposits of the Russian Platform), Leningrad: GNTI-NGTL, 1956, pp. 258–269.

Morozov, N.S., *Verkhnemelovye otlozheniya mezhdurech'ya Dona i Severnogo Dontsa i yuzhnoi chasti Volgo-Donskogo vodorazdela* (Upper Cretaceous Deposits in the Don–Severny Donets Interfluve and Southern Part of the Volga–Don Watershed), Saratov: Saratov. Gos. Univ., 1962 [in Russian].

Morozov, N.S. and Bondareva, M.V., Upper Cretaceous deposits of the Medveditsa–Volga interfluve within the Saratov Region, in *Voprosy geologii Yuzhnogo Urala i Povolzh'ya* (Problems of Geology of the Southern Ural and Volga Region), 1970, vol. 7, Pt. 1, pp. 116–141.

Morozov, N.S. and Orekhova, V.M., Cretaceous System. Upper Series, in *Geologiya SSSR. T. 46. Rostovskaya, Volgogradskaya, Astrakhanskaya oblasti i Kalmytskaya ASSR. Geologicheskoe opisanie* (Geology of the USSR. Vol. 46: Rostov, Volgograd and Astrakhan Oblasts and Kalmyk ASSR. Geological Description), Moscow: Nedra, 1969, pp. 318–361.

Naidin, D.P., *Verkhnemelovye belemnity Russkoi platformy i sopredel'nykh oblastei* (Upper Cretaceous Belemnites of the Russian Platform and Adjacent Areas), Moscow: Mosk. Gos. Univ., 1964 [in Russian].

Nekhrikova, N.I., The phylum Brachiopoda, in *Atlas bespozvonochnykh pozdnemelovykh morei Prikaspiiskoi vpadiny* (Atlas of Invertebrates from Late Cretaceous Seas of the Precaspian Depression), Moscow: Nauka, 1982, pp. 26–49.

Niebuhr, B., Baldschuhn, R., Ernst, E., Walaszczyk, I., Weiss, W., and Wood, C.J., The Upper Cretaceous Succession (Cenomanian–Santonian) of the Staffhorst shaft, Lower Saxony, Northern Germany: integrated biostratigraphic, lithostratigraphic and downhole geophysical log data, *Acta Geol. Polon.*, 1999, vol. 49, pp. 175–213.

Ogg, J., Ogg, G., and Gradstein, F.A., *Concise Geologic Time Scale: 2016*, Elsevier, 2016.

Olfer'ev, A.G. and Alekseev, A.S., *Stratigraficheskaya skhema verkhnemelovykh otlozhenii Vostochno-Evropeiskoi platformy. Ob"yasnitel'naya zapiska* (Stratigraphic Chart of the Upper Cretaceous Deposits of the East European Platform. Explanatory Note), Moscow: Paleontol. Inst. RAN, 2005 [in Russian].

Olfer'ev, A.G., Beniamovsky, V.N., Vishnevskaya, V.S., Ivanov, A.V., Kopaevich, L.F., Pervushov, E.M., Sel'tser, V.B., Tesakova, E.M., Kharitonov, V.M., and Shcherbinina, E.A., Upper Cretaceous deposits in the northwest of Saratov Oblast. Part 1: litho-and biostratigraphic analysis of the Vishnevoe Section, *Stratigr. Geol. Correl.*, 2007, vol. 15, no. 6, pp. 610–655.

Pervushov, E.M., Representatives of the genus *Cameraspongia* (Porifera, Hexactinellida) from the Cenomanian of the Volga River Region, *Izv. Saratov. Univ. Nov. Ser. Ser. Nauki o Zemle*, 2016a, vol. 16, no. 4, pp. 253–258. https://doi.org/10.18500/1819-7663-2016-16-4-253-258

Pervushov, E.M., Geochronology and structure of the Santonian "Sponge horizon" within the Volga right bank region, in *Melovaya sistema Rossii i blizhnego zarubezh'ya: problemy stratigrafii i paleogeografii. Sb. nauchn. tr.* (Cretaceous System of Russia and CIS Countries: Problems of Stratigraphy and Paleogeography. Coll. Sci. Works), Baraboshkin, E.Yu., Ed., Simferopol: Izd. dom "Chernomorpress", 2016b, pp. 205–207.

Pervushov, E.M., The genus *Balantionella* (Porifera, Hexactinellida), *Izv. Saratov. Univ. Nov. Ser. Ser. Nauki o Zemle*, 2018, vol. 18, no. 2, pp. 122–134.

Pervushov, E.M., Sel'tser, V.B., Kalyakin, E.A., Fomin, V.A., Ryabov, I.P., Il'inskii, E.I., Gujikova, A.A., Biryukov, A.V., and Surinskiy, A.M., Integrated bio- and magnetostratigraphic study of the "Ozerki" Sections (Upper Cretaceous, Volga River right bank, Saratov Region). Paper 1. Section characteristics, results of petromagnetic and magnetic–mineralogical examinations, *Izv. Saratov. Univ. Nov. Ser. Ser. Nauki o Zemle*, 2017a, vol. 17, no. 2, pp. 105–116. https://doi.org/10.18500/1819-7663-2017-17-2-105-116

Pervushov, E.M., Sel'tser, V.B., Kalyakin, E.A., Fomin, V.A., Ryabov, I.P., Il'inskii, E.I., Guzhikova, A.A., Biryukov, A V., and Surinskiy, A.M., Integrated bio- and magnetostratigraphic study of the "Ozerki" sections (Upper Cretaceous, Volga River right bank, Saratov Region). Paper 2. Oryctocoenosis characteristics and biostratigraphy, *Izv. Saratov. Univ. Nov. Ser. Ser. Nauki o Zemle*, 2017b, vol. 17, no. 3, pp. 182–199. https://doi.org/10.18500/1819-7663-2017-17-3-182-199

Pettitt, N., A monograph on the Rhynchonellidae of the British Chalk. Pt. 2, *Palaeontogr. Soc. Monogr. (London)*, 1954, vol. 107, pp. 27–52.

Rykov, S.P., The Upper Cretaceous stratigraphy of the Medveditsa River basin, *Uch. Zap. Saratov. Gos. Univ., Vyp. Geol.*, 1951a, vol. 28, pp. 84–93.

Rykov, S.P., On the problem of the Mesozoic stratigraphy of the northern part of the Doskaya Luka locality, *Uch. Zap. Saratov. Gos. Univ., Vyp. Geol.*, 1951b, vol. 28, pp. 158–164.

Sadekov, A.Yu. and Beniamovsky, V.N., Stratigraphic role of species of the genus *Stensioeina* (benthic foraminifers), phylogenetic evolution and its palaeobiogeography in the Turonian-Santonian of the East Europe and adjacent Mangyshlak Peninsula, in *Proc. 7th Micropaleontol. Workshop Micro-2009, Sw. Katarzyna, Poland, September 28–30, 2009. Abstracts and Excursion Guide, Grzybowski Foundation Spec. Publ.*, Warsawa, Poland, 2009, no. 15, pp. 64–65.

Saltykov, V.F. and Pervushov, E.M., The local stratigraphic subdivisions of the Upper Cretaceous in the Tersa depression (Volgograd Region), in *Sb. nauchn. tr. "Melovaya sistema Rossii i blizhnego zarubezh'ya: problemy stratigrafii i paleogeografii"* (Coll. Sci. Works "Cretaceous System of Russia and CIS Countries: Problems of Stratigraphy and Paleogeography"), Pervushov, E.M., Ed., Sartatov: Saratov. Gos. Univ., 2007a, pp. 204–221.

Saltykov, V.F. and Pervushov, E.M., The structure of the Bannovka Formation and its relationships with adjacent Upper Cretaceous stratotype sections in the north of the

Tersa depression (Volgograd Region), *Izv. Vuzov. Geol. Razved.*, 2007b, no. 5, pp. 8–13.

Sedaikin, V.M., Bedrina,T.A., Bondareva, M.V., and Samsonov, V.F., The Upper Cretaceous deposits in the area of Tavricheskii settlement (Saratov Trans-Volga Region), in *Voprosy geologii Yuzhnogo Urala i Povolzh'ya. Vyp. 6* (Problems of Geology of the Urals and Volga Region. Vol. 6), Saratov: Saratov. Gos. Univ., 1969, pp. 163–174.

Sel'tser, V.B., Kalyakin, E.A., Il'inskii, E.I., and Ryabov, I.P., The Coniacian–Santonian fauna from the northeastern part of the Pavlovsk Arch of the Voronezh anteclise (Voronezh Region). Preliminary data, in *Mat. Nauchn. Mezhved. konf. "Geologicheskie nauki-2017"* (Proc. Sci. Interdepart. Conf. "Geological Sciences–2017"), Saratov: Izd. "Tekhno-Dekor", 2017, pp. 42–43.

Semenov, V.P., Stratigraphy of the Upper Cretaceous deposits in the Middle Don region between Kazanskaya and Elanskaya cossack villages, in *Tr. Voronezh. Gos. Univ.* (Trans. Voronezh State Univ.), 1959, vol. 50, pp. 86–91.

Sklenar, J. and Simon, E., Brachiopod Gyrosoria Cooper, 1973 – a comparative palaeoecological, stratigraphical and taxonomical study, *Bull. Geosci.*, 2009, vol. 84, no. 3, pp. 437–464.

Smirnov, Yu.P. and Pergament, M.A., Coniacian Stage in Dagestan: composition and zonal subdivision, in *Tr. Vsesoyuzn. kollokviuma po inotseramam. Vyp. 1.* (Proc. All-Union Inoceram Coll. Vol. 1), Moscow: Geol. Inst. RAN, 1972, pp. 146–156.

Smith, A.B. and Wright, C.W., British Cretaceous echinoids. Part 4. Stirodonta 3 and Camarodonta, *Monogr. Palaeontograph. Soc. London*, 1996, vol. 150 (602), pp. 286–341.

Sobetskiy, V.A., Bottom assemblages and biogeography of Late Cetaceous platform seas in the southwestern USSR, in *Tr. PIN. T. 166* (Trans. Paleontol. Inst. Vol. 166), Moscow: Nauka, 1978.

Storc, R. and Zitt, J., Late Turonian ophiuroids (Echinodermata) from the Bohemian Cretaceous Basin, Czech Republic, *Bull. Geosci.*, 2008, vol. 83, pp. 123–140.

Stratigraficheskaya skhema verkhnemelovykh otlozhenii Vostochno-Evropeiskoi platformy (Stratigraphic Scheme for the Upper Cretaceous Deposits of the East European Platform), St. Petersburg: Kartogr. Fabr. Vseross. Nauchno-Issled. Geol. Inst., 2004 [in Russian].

Surinskiy, A.M. and Guzhikov, A Yu., Experience of cyclostratigraphic analysis of petromagnetic data on the Turonian–Maastrihtian section "Nizhnyaya Bannovka" (Volga River right bank, Southern Saratov Region), *Izv. Saratov. Inst. Nov. Ser. Ser. Nauki o Zemle*, 2017, vol. 17, no. 2, pp. 117–124. https://doi.org/10.18500/1819-7663-2017-17-2-117-124

Taboyakov, A.Ya., The paleontological characteristics of the Emscherian deposits from the Donskaya Luka locality, in *Uch. zap. Saratov. Gos. Univ. im. N.G. Chernyshevskogo* (Trans. Chernyshevsky Saratov State Univ.), 1953, vol. 38.

Tarling, D.H. and Hrouda, F., *The Magnetic Anisotropy of Rocks*, Chapman & Hall, 1993.

Vasilenko, V.P., Anomalinids, in *Iskopaemye foraminifery SSSR* (Fossil Foraminifers of the USSR), Leningrad: Gostoptekhizdat, 1954 [in Russian].

Vasilenko, V.P., Upper Cretaceous foraminifers of the Mangyshlak Peninsula, in *Tr. VNIGRI. Vyp. 171* (Trans. All-Russ. Petrol. Res. Inst. Vol. 171), 1961

Vishnevskaya, V.S., *Radiolyarievaya biostratigrafiya yury i mela Rossii* (Radiolarian Biostratigraphy of the Jurassic and Cretaceous of Russia), Moscow: GEOS, 2001 [in Russian].

Vishnevskaya, V.S. and Djerič, N., Mesozoic Radiolaria of Bosnia and Serbia: new data, *Paleontol. J.*, 2009, vol. 43, no. 12, pp. 1513–1569.

Vishnevskaya, V.S., Kopaevich, L.F., Beniamovsky, V.N., and Ovechkina, M.N., The correlation of the Upper Cretaceous zonal schemes of the Eastern European Platform based on foraminifera, radiolaria, and nannoplankton, *Moscow Univ. Geol. Bull.*, 2018, vol. 73, no. 2, pp. 131–140.

Walaszczyk, I. and Peryt, D., Inoceramid–foraminiferal biostratigraphy of the Turonian through Santonian deposits of the Middle Vistula Section, Central Poland, *Zentralbl. Geol. Paläontol.*, 1998a, nos. 11/12, pp. 1501–1513

Walaszczyk, I. and Wood, C.J., Inoceramids and biostratigraphy at the Turonian/Coniacian boundary; based on the Sazgitter-Salder Quarry, Lower Sxony, Germany, and the Słupia Nadbrzeżna section, Central Poland, *Acta Geol. Polon.*, 1998b, vol. 48, no. 4, pp. 395–434.

Walaszczyk, I., Kopaevich, L.F., and Olferiev, A.G., Inoceramid/foraminiferal succession of the Turonian and Coniacian (Upper Cretaceous) of the Briansk Region (Central European Russia), *Acta Geol. Polon.*, 2004, vol. 54, no. 4, pp. 597–609.

Walaszczyk, I., Wood, C.J., Lees, J.A., Peryt, D., Voigt, S., and Wiese, F., The Salzgitter–Salder Quarry (Lower Saxony, Germany) and Słupia Nadbrzeżna river cliff section (central Poland): a proposed candidate composite Global Boundary Stratotype Section and Point for the base of the Coniacian Stage (upper Cretaceous), *Acta Geol. Polon.*, 2010, vol. 60, no. 4, pp. 445–477.

Walaszczyk, I., Kopaevich, L.F., and Beniamovsky, V.N., Inoceramid and foraminiferal record and biozonation of the Turonian and Coniacian (Upper Cretaceous) of the Mangyschlak Mts., western Kazakhstan, *Acta Geol. Polon.*, 2013, vol. 63, no. 4, pp. 469–487.

Translated by N. Astafiev